BESSY

Berliner Elektronenspeicherring-Gesellschaft
für Synchrotronstrahlung m.b.H.

STARS

Proposal for the Construction of a Cascaded HGHG FEL

Berlin, October 2006

The STARS Design Group

M. Abo-Bakr, W. Anders, J. Bahrdt, K. Bürkmann, P. Budz, O. Dreßler, H. Dürr, V. Dürr, W. Eberhardt, S. Eisebitt, J. Feikes, R. Follath, A. Gaupp, R. Görgen, K. Goldammer, S. Heßler, K. Holldack, E. Jaeschke, T. Kamps, S. Klauke, J. Knobloch, O. Kugeler, B. Kuske, P. Kuske, D. Krämer[1], F. Marhauser, A. Meseck, R. Mitzner, R. Müller, A. Neumann, M. Neeb, K. Ott, D. Pflückhahn, T. Quast, M. Scheer, T. Schroeter, M. Schuster F. Senf, G. Wüstefeld

Editors

J. Knobloch, E. Jaeschke, W. Eberhardt

[1] Now at GSI, Darmstadt

1 Introduction

In March 2004, the Berliner Elektronenspeicherring-Gesellschaft für Synchrotronstrahlung (BESSY) published the Technical Design Report (TDR) [1] for a Soft X-ray Free Electron Laser (FEL) user facility in the photon energy range from 24 eV to 1000 eV, based on the High-Gain Harmonic-Generation (HGHG) principle. This scheme of cascading seeded FEL stages offers the only possibility to generate photon pulses of variable femtosecond duration, gigawatt peak power, full shot-to-shot pulse reproducibility, wide-range tunability and full transverse and longitudinal coherence. The BESSY user community is convinced that only a HGHG 2nd generation FEL will be able to fulfill all of these crucial requirements for the next generation of experiments.

In 2005 the TDR was presented to the Working Group on Large-Scale Facilities for Fundamental Scientific Research of the German Science Council and received excellent marks. The following is an extract from the Council's Evaluation Statement [2]:

"*The programme is at the forefront of international research and will have a strong impact on basic as well as applied science. The enhanced technical approach with the seeding scheme (HGHG) will further strengthen and broaden the scientific programme in significant areas. The specific characteristics of the BESSY FEL will allow gaining insight in particular by making use of the*

- *reproducible pulse structure and peak intensity,*
- *high time resolution,*
- *complete transverse and longitudinal coherence (transform limited pulses),*
- *energy tunability by changing the seeding pulse and/or undulator gap,*
- *synchronized pump-and-probe experiments,*
- *high repetition rate (CW-operation).*"

As a result, the Science Council ranked the BESSY project in its Category 2 (*"recommended for realization under conditions"*), the condition being that a two-stage HGHG *cascade* be demonstrated in an R&D program spanning 3 to 4 years.

BESSY has taken up this recommendation and presents with this document the proposal for the proof of principle facility STARS for cascading HGHG stages. Following the advice of the Science Council, other important topics for the BESSY FEL such as CW-operation and development of SRF gun technology will also receive close attention in the R&D program.

Many of the components and technical issues for STARS are identical or very similar to those of the BESSY FEL. Hence this proposal is designed to provide a general overview of the main components of STARS. For further details, the reader is frequently referred to the TDR [1] of the BESSY FEL.

The STARS design group has benefited greatly from discussions, comments and suggestions made by colleagues from Germany (DESY, MBI, TU-Darmstadt, TU-Dresden) as well as from abroad (ALS, APS, BNL, Cornell, ELETTRA, ESRF, INFN Milano, JLab, Maxlab, MIT Bates, CEA Saclay, SLAC, IPN Orsay and UCLA). Their contributions were invaluable for the completion of this document just as for the TDR.

2 Principle of HGHG

Ultra-short pulses from single-pass free electron lasers are the tools for future time resolved experiments. Whereas the SASE approach produces short wavelength light at high peak power with an excellent spatial mode, the poor temporal coherence and the intrinsic chaotic shot-to-shot variations of the pulse made the development of alternative approaches mandatory. In the High-Gain-Harmonic-Generation (HGHG) process, pioneered and successfully demonstrated at BNL by L.H. Yu and co-workers, the light output is derived from a coherent sub harmonic "seed" field. HGHG cascades are then used to convert the seed laser wavelength to the desired spectral range. For example, the BESSY Soft X-ray FEL will use four stages to reach photon energies up to 1 keV.

The underlying idea of the HGHG process depicted in Figure 2.1 is to overlap the electron bunch with the field of an external high-power seed laser in a short undulator tuned to be in resonance with the laser according to the well known relationship

$$\lambda = \lambda_u \frac{1+K^2}{2\gamma^2}, \qquad (1)$$

where λ is the radiation wavelength, γ the relativistic factor of the electrons, λ_u the undulator period and K the RMS undulator parameter proportional to the magnetic field strength of the undulator.

In the first magnet structure, called the modulator, the seed field interacts with the electron beam, thereby introducing an energy modulation. The beam then passes through a dispersive section, e.g., a three-dipole chicane, where the energy modulation is converted into a spatial modulation.

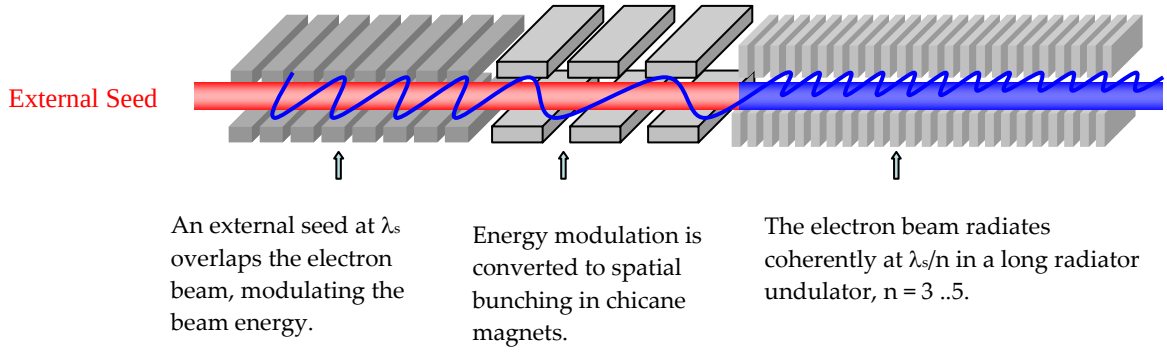

Figure 2.1: Principle of the HGHG scheme

Given a sufficiently high seed peak power, the phase information of the seed laser is imprinted on the density modulated electron beam because it dominates the shot noise. Abundant harmonics of the seed frequency exist in the modulated beam which are exploited as the beam enters the next section, the radiator. This is tuned to be resonant to

one of these higher harmonics, e.g., λ/3 or λ/5. Coherent emission at this higher harmonic is produced and can be exponentially amplified until saturation is achieved. Ideally the HGHG output radiation is Fourier-transform-limited since it is also longitudinally completely coherent.

The main advantage of the HGHG scheme is that the properties of the output radiation at the harmonic wavelength are a "map" of the characteristics of the high-quality fundamental seed laser field. This includes a high degree of stability, the bandwidth, the output power, the shape, the duration of the output pulse, and the intrinsic possibility to synchronize the user experiments. Since the seed pulse can be made much shorter than the electron bunch, the output pulse duration is no longer determined by the bunch length but rather by the seed laser. This is one of the main advantages over SASE-type FELs, where the output pulse is determined by the electron bunch length. Thus, an HGHG FEL maintains the flexibility of the high-power seed laser.

For a machine such as the BESSY FEL, harmonics up to approximately 5th order can be exploited. To reach even shorter wavelengths, the output of an HGHG stage can be again used to seed a further HGHG stage, as shown in Figure 2.2. By cascading multiple stages one can thus reach shorter and shorter wavelengths. For the best efficiency of up-conversion in an HGHG stage it is, however, important to provide a fresh part of the electron bunch that interacts with the seed field. Hence one needs to use a relatively long bunch and introduce a delay between the electrons and the seed field between stages to prevent the seed from interacting with a portion of the bunch that has already been disturbed in a previous stage. This "fresh-bunch" technique was proposed by Ben-Zvi, Yang and Yu [3].

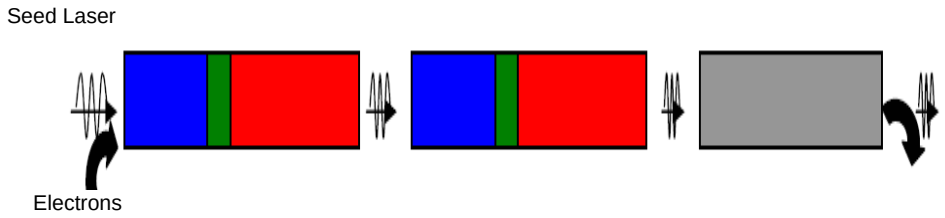

Figure 2.2: Principle of HGHG cascading for two stages and a final amplifier. Blue = modulator, green = dispersive section, red = radiator, gray = final amplifier.

Cascading HGHG stages is the basic concept of the BESSY Soft X-ray FEL and has been extensively investigated by simulations (see Chapter 3 of the TDR). So far, cascading has not been demonstrated experimentally. Hence the proposed R&D phase and construction of STARS is of utmost importance not only for the BESSY FEL but for the FEL community as a whole. STARS will be the first proof-of-principle experiment for a two-stage HGHG cascade.

3 Layout of STARS

The proof-of-principle facility STARS will be set up in an extension of the existing heavy equipment hall (SLH) at BESSY (Figure 3.2) that houses the cavity test facility HoBiCaT and the undulator development and fabrication shop. The extension will be placed between the storage ring building and the SLH in such a way, that the facility can remain fully operational even once the BESSY Soft X-ray FEL has been commissioned.

STARS is planned for lasing in the wavelength range 40-70 nm (fundamental power), requiring a beam energy of approximately 325 MeV and a peak current of 500 amperes. A schematic of the STARS layout is shown in Figure 3.1. A normal conducting photo-injector gun generates high quality bunches (projected emittance 1.7 π mm mrad at 1 nC) at repetition rates up to 100 Hz. Three superconducting TESLA-type cryomodules, modified for CW operation, then boost the energy to 325 MeV. These contain twenty 9-cell TESLA type cavities, the last cryomodule being filled with only four cavities, allowing for an energy upgrade at a later time. A bunch-compressor section is placed between the second and the third module. To linearize the RF potential of the linac for efficient bunch compression, a third-harmonic-cavity section is also included before the bunch compression section. The last superconducting module is followed by a collimator to protect the downstream HGHG cascade.

The major systems of STARS are discussed in the following sections:

- A high brilliance photo-injector: Section 4
- The superconducting CW linear accelerator: Section 5
- The bunch compressor: Section 6
- The HGHG undulator cascades: Sections 7 & 8
- Diagnostics for electron and photon beams: Section 9
- Endstation for an evaluating experiment: Section 10
- Conventional infrastructure facilities: Section 11

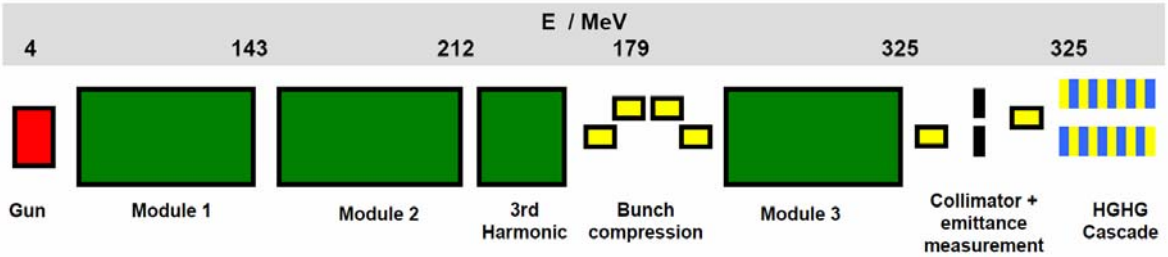

Figure 3.1: Layout of the main components of STARS.

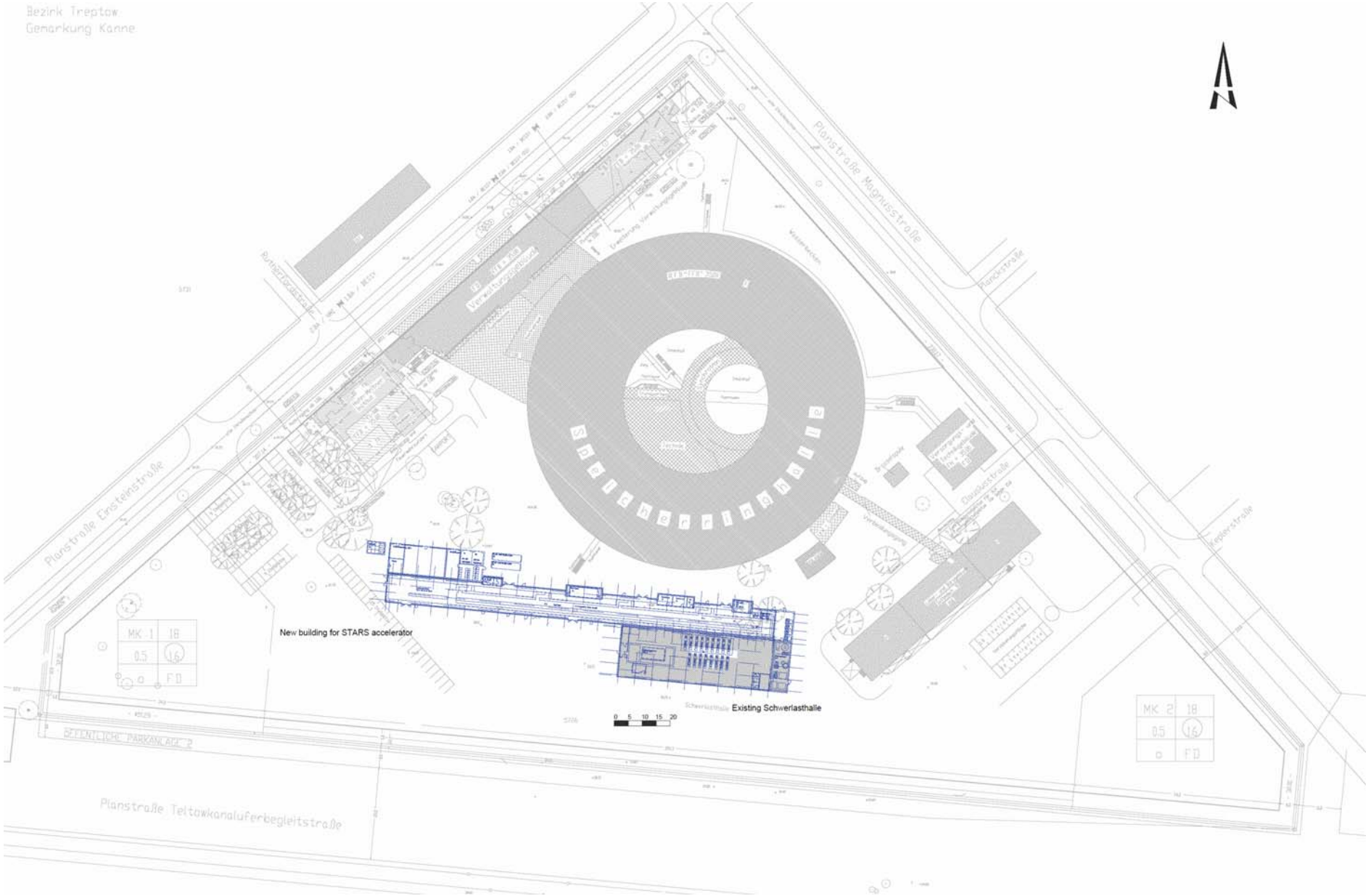

Figure 3.2: Location of the STARS facility on the BESSY site in Berlin, Adlershof.

4 The Electron Injector

4.1 Photoinjector Layout

A normal-conducting 1.3 GHz RF photoinjector will deliver the high-brightness electron beam required for STARS. A *slice* beam emittance of 1.5 π mm mrad at a bunch charge of 1 nC and peak current of 500 A is required at the FEL. However space-charge effects limit the operating peak current of the gun to about 30 and hence subsequent bunch compression at higher energy will be required.

Photoinjector development suitable for future FELs has been pursued strongly since 2000 by the PITZ collaboration at DESY-Zeuthen, of which BESSY is a founding member. At PITZ, a *projected* beam emittance of 1.6 π mm mrad at 1 nC has already been demonstrated [4]. Given BESSY's extensive experience in operating the PITZ gun, the STARS system will be strongly modeled on this.

A schematic of the photogun is shown in Figure 4.1. A UV drive laser ($\lambda = 262$ nm) illuminates a cesium-telluride (Cs_2Te) photocathode to release electron bunches of 20 ps length. The cavity operates at an electric field of 40 MV/m to quickly boost the beam to relativistic energies and overcome the space-charge effects as soon as possible. Emittance dilution due to space-charge forces along the bunch is compensated by applying an external magnetic field from a solenoid (emittance compensation [5]). The solenoid produces a beam waist where the entrance of the subsequent superconducting linear accelerating module is positioned to further accelerate the beam to ultra-relativistic energies and to freeze the emittance. To properly match the beam delivered by the gun to the linac, the field gradient in the linac cavities is chosen according to the invariant envelope criterion [6]. Related details on the beam dynamics are extensively described in the TDR.

The STARS photoinjector will initially be operating at a repetition rate of 100 Hz, with the option to increase this to 1 kHz at a later stage. Given an RF pulse length of 25 μs, the duty factor is 0.25%, less than the 1% used at both PITZ and FLASH. Thermal loading (7.5 kW) will therefore not be an issue, in fact the reduced load with short pulses improves the stability of the RF system. If 1-kHz operation is realized at a later date, the thermal loading will increase to 75 kW. To handle this, the cooling of the PITZ gun was improved and a prototype of the new design was recently tested successfully at PITZ to 47 kW power dissipation (limited by the available RF power at the gun) and 51 MV/m accelerating field [7]. The setup used for the test is shown in Figure 4.2.

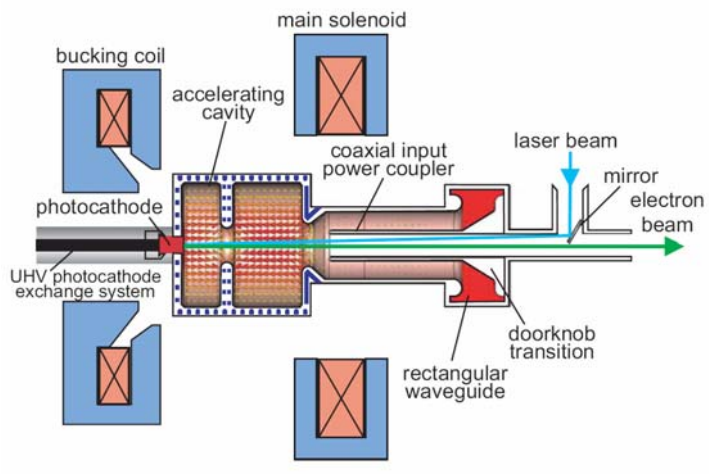

Figure 4.1: Schematic of the 1½-cell laser-driven normal-conducting RF gun showing the coaxial input coupler and solenoids for emittance compensation.

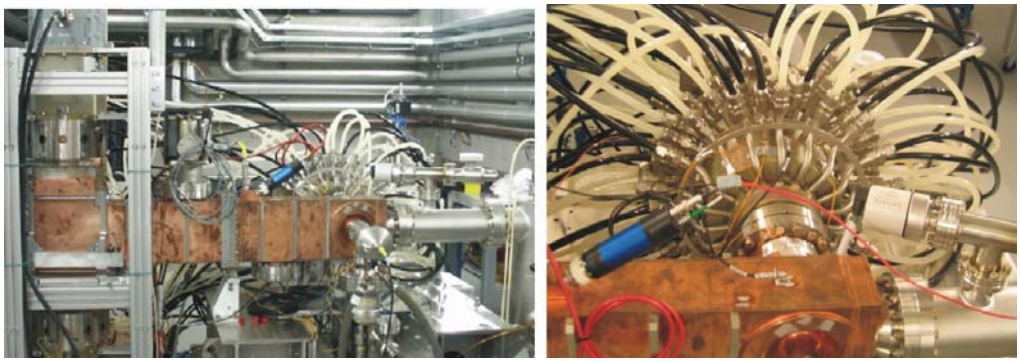

Figure 4.2 RF cavity test stand at PITZ (left) and close-up of the cavity with cooling water circuitry.

4.2 RF Gun Modulator

The STARS requirements for the photoinjector RF system are the same as for the BESSY FEL, except that the repetition rate has been relaxed from 1 kHz to 100 Hz. Thus, all components for the STARS injector could be used directly for the BESSY FEL.

A pulsed modulator power supply will feed the klystron and the RF power is transferred by waveguide and circulator to the gun cavity. For eventual 1 kHz operation, a fast amplitude feedback loop can be used to reduce the filling time of the cavity to reduce the thermal load below the 75 kW for which the cavity was designed.

As discussed in the TDR Chapter 5, the klystron requirements are well within the current technological limits. Units exist at higher and lower frequencies producing significantly more power. A power of 4 MW is needed for 40 MV/m operation of the gun, which is easily achieved by the Thales TH2104U klystron.

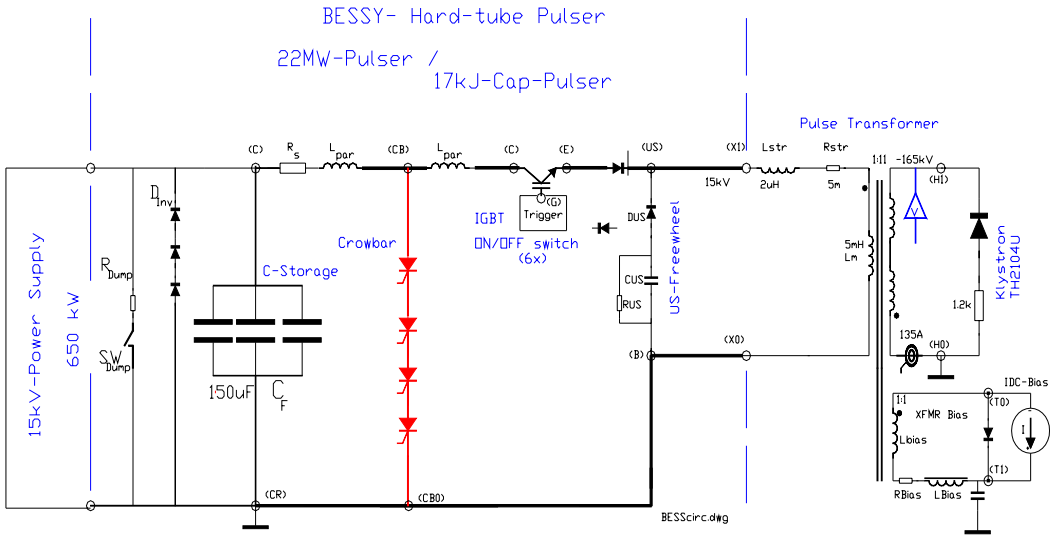

Figure 4.3: Hard-tube modulator for the normal-conducting gun cavity.

Various modulator designs have been investigated and a hard-tube modulator, as shown in Figure 4.3, has been chosen for its flexibility, stability and reasonable cost. A bank of capacitors is charged by a set of 15 kV power supplies in parallel, the number determining the repetition rate. Part of the energy is transferred by an on/off IGPT switch to a pulse transformer, the length being determined by the trigger pulse.

4.3 RF Control

RF control of the gun field is critical to provide stable shot-to-shot beam parameters. Generally, an important source of jitter are thermal drifts in the gun body. However, given the relatively low thermal loading and short-pulse operation the impact of drifts is small. Furthermore an improved cooling layout, in conjunction with water temperature control at the 0.1 °C level alone will provide for phase stabilization better than 2 degrees. This is improved considerably by the use of a fast feedback system with loop delays less than 1 μs. It employs a feedback signal provided by a field pickup probe integrated in the gun that yields a direct measurement of the achieved field stability.

4.4 Gun Laser System

The general layout for the photocathode laser for STARS is very similar to that of the BESSY FEL described in the TDR, Chapter 5. For STARS the requirements are less stringent because the use of single pulses instead of pulse trains and a diminished repetition rate of only 100 Hz reduce the average power significantly. Hence the thermal load on all components is lower resulting in a simpler and more stable setup.

Beam-dynamics simulations for STARS have shown that a flat-top profile is desirable to optimize the beam emittance and hence the HGHG output quality. To extract a charge of 1 nC, calculations have shown that the emittance is minimized for a flat-top length of approximately 20 ps (see TDR, Chapter 5). On the other hand, in STARS the beam quality is relatively insensitive to the laser-pulse rise time, and values of order 6 ps are fully sufficient. Hence, a standard diode-pumped laser based on Nd:YLF laser material will be installed. The building blocks for this type of laser are already fully developed and have been operated very successfully for photocathode lasers at FLASH (DESY/Hamburg) and at PITZ [8]. Typically, such a system can produce flat-top laser profiles with the required rise times on the order of 6-8 ps.

Another advantage of the Nd:YLF system lies in the fact that a system capable of producing Gaussian bunches can be installed quickly and at an early stage of STARS construction. It can then be used for the commissioning of the injector and later the full linac. Only once the full HGHG experiments are carried out, does its upgrade with a pulse-shaper for full flat-top operation have to be complete. If needed, a spatial flat-top profile in the transverse plane can be produced by imaging an over-illuminated pinhole onto the photocathode.

Even shorter rise times are feasible with other laser mediums such as Yb:KGW and Yb:YAG. In a test setup at the Max-Born-Institute a minimal slope of 1.5 ps is presently achieved with Yb:KGW [9]. Such a system may be considered for a future upgrade of STARS. The parameters of this laser will be a pulse with a minimum rise/falltime of 1.5 ps and a flat top of 20 ps in the UV (~260 nm). It provides ample energy to extract the required bunch charge of 1 nC.

5 The Superconducting CW Linac

Superconducting RF technology developed by the TESLA collaboration and as described in Chapter 6 of the TDR has been chosen for the CW linear accelerator of the BESSY FEL. Figure 5.1 shows a photo of the "standard" TESLA module. This choice is driven by the fact, that the technology is mature and has been operated very reliably for a number of years.

This technology will therefore also be adopted for STARS. There are further, compelling reasons for this choice:

- The linac will operate under near-identical conditions as the BESSY FEL and thus can serve as an ideal test bed for the modifications that need to be made to adapt the pulsed TESLA technology for CW operation.
- Production of TESLA-type modules can occur in close collaboration with DESY to yield significant cost and time savings. Also, one can take advantage of the technology transfer to industry that is already under way.
- BESSY personnel can be trained at an early stage in handling and operating superconducting RF accelerating units.
- The operation of a medium-size cryogenic plant will provide valuable insight into the future specification of the cryoplant for the BESSY FEL.

Figure 5.1: A TESLA cryo-module that will be the basis of both the STARS and BESSY FEL linacs.

The changes required for CW operation are discussed in detail in the TDR, Chapter 6. To confirm their suitability for reliable CW operation, BESSY has already worked on an intensive qualification program. Tests of couplers [11] and tuners [12] and important studies of cryogenic parameters, such as the optimum bath temperature required for reliable and economic CW operation, have been performed. The Horizontal Bi-Cavity

Test facility HoBiCaT (Figure 5.2) has been set up for this purpose, and has been used extensively for R&D on superconductive CW cavities.

The HoBiCaT facility will play a crucial role for the BESSY Soft X-ray FEL project, and it has already taken up a leading position in the CW SRF development program in Europe within the context of the EuroFEL collaboration.

5.1 Operational Parameters

5.1.1 Accelerating Field

Simulations of the HGHG scheme have shown that a beam energy of 325 MeV is sufficient for lasing at a wavelength down to 40 nm. This energy can be reached comfortably with three TESLA-type modules containing a total of 20 cavities. Ideally all cavities will operate at the same nominal voltage. Hence, given an injection energy of 4 MeV out of the photoinjector and an acceleration phase of 14 degrees before the bunch compressor, the cavities need to be operated at 17.2 MV/m, which lies well within the currently achieved performance. Note that this value takes into account a total decelerating voltage of about 30 MeV in the third harmonic section (see Section 6).

5.1.2 RF Power

At 1 nC bunch charge and a repetition rate of 100 Hz, beam loading in STARS is negligible (< 2 W per cavity). RF power therefore will be needed primarily to compensate the microphonic detuning in the cavities. The RF system for the BESSY FEL was laid out for peak microphonics up to 42 Hz to reduce the anticipated trip rate to less than one a day.

Figure 5.2: The BESSY Horizontal Bi-Cavity Test-facility (HoBiCaT).

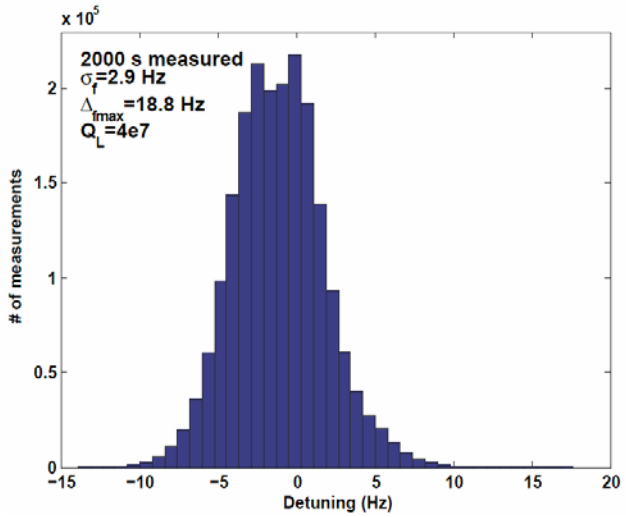

Figure 5.3: Distribution of microphonic detuning measured in HoBiCaT.

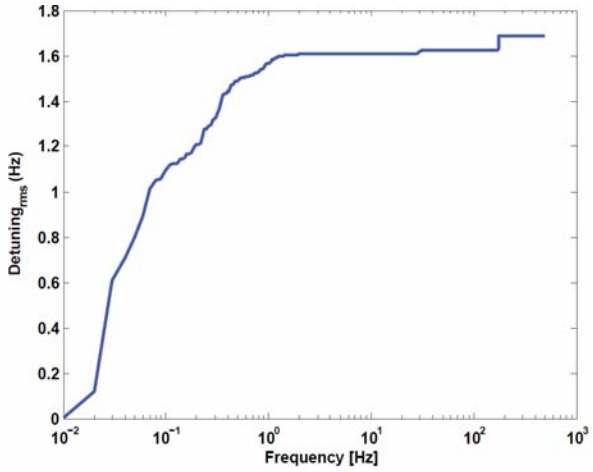

Figure 5.4: Cumulative spectrum of microphonic detuning measured in HoBiCaT (not measured at the same time as Figure 5.3).

Measurements in HoBiCaT have shown that RMS microphonics are of order 3 Hz or less with peak excursions around 15 Hz (Figure 5.3). A significant portion of these microphonics are at frequencies below 1 Hz (Figure 5.4) and are caused by pressure fluctuations in the helium gas-return system, of order 0.03 mbar RMS. Means to reduce these are being investigated, but it is anticipated that the large volume of the STARS helium system will reduce the RMS fluctuations further. Even if this is not the case, active compensation of these pressure fluctuations by means of the cavity's piezo-tuner can be employed and have already been tested successfully in HoBiCaT.

Hence, for STARS the RF system will be dimensioned to handle microphonic detuning values of 5 Hz RMS and 25 Hz peak. The optimal bandwidth then is 50 Hz, or an external coupling of 2.6×10^7. At 17.2 MV/m accelerating field this translates into an RF power requirement of

P_{ave} = 3.1 kW

P_{peak} = 5.9 kW.

As was already demonstrated in HoBiCaT, these values are within the thermal capabilities of the standard TTF-III coupler, even if it is not modified for additional cooling [11]. Should a cavity need to be operated at a higher gradient, e.g., 20 MV/m, the peak and average power requirements increase to 8 kW and 4.2 kW, respectively, still within range of the standard coupler system.

5.1.3 Bath Temperature

Operation of the cryogenic plant is expected to be at 1.8 K, based on recent measurements of the cavity quality factor versus temperature in HoBiCaT (Figure 5.5). These measurements demonstrated that the cavity quality continues to improve significantly as the temperature is lowered below 2 K. Experience with HoBiCaT has shown that stable operation at 1.8 K is possible, so that one may take advantage of the reduced cryogenic load by lowering the bath temperature.

Given the fact that the magnetic shielding of a TESLA-type module is not as good as HoBiCaT's (which has a double shield) and that at high field electron emission may play a role, a quality factor of 3×10^{10} will unlikely be attained in all cavities. For the dimensioning of the cryoplant and to include a safety margin, a quality factor of

$$Q_0 = 1.4 \times 10^{10}$$

is therefore assumed. For cavity operation at 17.2 MV/m each cavity will therefore dissipate P_{diss} = 22 W, similar to what is planned for the BESSY FEL.

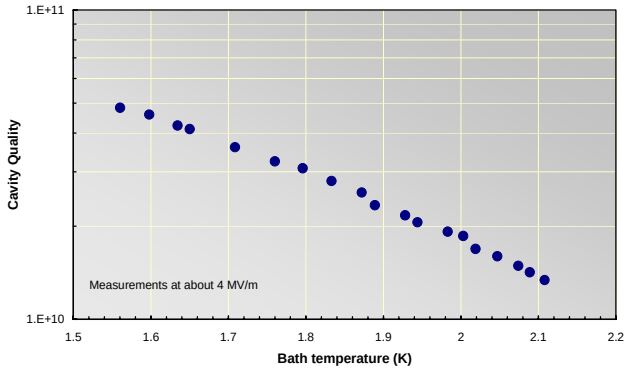

Figure 5.5: Low-field measurement of the cavity quality versus temperature of a TESLA-type cavity in HoBiCaT.

5.2 Third Harmonic Cavity

Third harmonic cavities are required for the linearization of the accelerating voltage for efficient bunch compression (see Section 6). Such a system is currently under

development by FermiLab and DESY, this being based on a scaled version of the TESLA cavities. The cryostat represents a shorter version of the accelerating modules and attaches directly to Module 2 in STARS (no warm transition).

Installation of the first 3rd harmonic system is planned for FLASH in 2007 [10]. Similar to the 1.3-GHz system, the harmonic cavities and associated coupler design will need to be adapted for CW operation. Tests will be performed in the HoBiCaT facility.

5.3 RF System

5.3.1 RF System for Accelerating Cavities

The RF system will be identical to the one planned for the BESSY FEL (see TDR Chapter 6). The STARS system will consist of 20 individual transmitters supplying one cavity each with up to 10 kW RF power via coaxial transmission lines. Vector-sum operation of several cavities, as in FLASH, is not a suitable alternative, because for narrow-bandwidth (low-beam-loading) operation, the required field stability cannot be achieved. Furthermore, powering each cavity with its own transmitter provides significantly more flexibility and reliability.

10 kW RF power is sufficient for 20 MV/m operation, given peak microphonic detuning around 25 Hz and negligible beam loading. To account for distribution-line losses and a safety factor, the transmitter must therefore provide 15 kW. Due to the fact, that the power level is dominated by the microphonic detuning, the *average* power level is below 5 kW.

The main components of the transmitter are: The RF power tube (IOT), the DC-power supplies, the coaxial RF power cable, waveguides and circulator, the interlock system and the low-level RF-control system providing the required stability.

Prototype development for a suitable transmitter is already under way at the HoBiCaT facility. Figure 5.6 shows the first system with a klystron and an IOT prototype. A dedicated power supply for the IOT will be available in late 2006 for initial IOT transmitter tests. A cost optimized version will then be developed in 2007.

Similarly, prototyping of the low-level RF-control system is well under way at the HoBiCaT facility. RF control will be provided by a digital, FPGA-based, system as described in Chapter 6 of the TDR. The stability requirements for the STARS main linac are somewhat relaxed compared to the BESSY FEL because the bunch compression factor is only 11 rather than 30 in the BESSY FEL. Hence the translation of field errors into timing jitter by the bunch compressors is not as severe.

5.3.2 Third Harmonic RF system

A similar transmitter layout as for the accelerating cavities will be used for the 3rd harmonic frequency, albeit at a lower power rating. About 1.5 kW per cavity will be

required. At 3.9 GHz, IOT tubes are not available and a klystron as the power tube is the best choice. A pulsed system is already commercially available, with only minor changes required for CW operation. Waveguide transmission lines will be used to transfer the power to the cavities.

Figure 5.6: First HoBiCaT transmitter prototype: in the middle the power supply, right side the 10 kW klystron and left side an IOT prototype.

5.4 Cryogenics

As described in the TDR Chapter 15, the accelerating cavities of STARS are cooled with superfluid He II at 1.8 K. The cold helium is provided by two medium-size cryogenic plants which are part of the BESSY-II installation. A 1.8-K sub-cooling unit must be installed for STARS. The requirements are listed in Table 5.1.

Table 5.1: Cryogenic losses of the superconducting linac

Temperature	Purpose	Static losses	Dynamic losses	Total losses
1.8 K	Cavity losses	21 W	602 W	623 W
5/8 K	Shield cooling	74 W	48 W	122 W
40/80 K	Shield cooling	560 W	520 W	1080 W

The size and also the costs of the installation are dominated by the cooling capacity at the 1.8 K temperature level. Due to CW operation, nearly all losses at 1.8 K are dynamic losses of the cavities.

5.4.1 Cryogenic Distribution

The 20 cavities in the superconducting linac are grouped into three modules. Two of these contain eight cavities each. The third module houses only four cavities with the remaining four being replaced by blank tubes to preserve the well established cryostat design. These may be replaced at a later date by cavities for an energy upgrade of STARS. The third harmonic cavities will be housed in a separate, dedicated module.

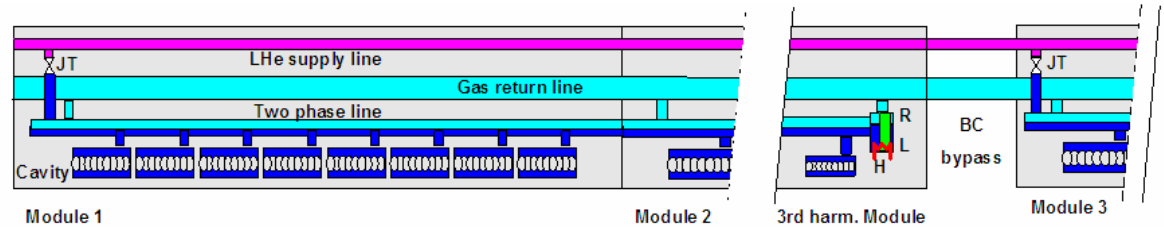

Figure 5.7: Design concept for the BESSY FEL cryogenic module (JT: Joule-Thomson valve, R: reservoir, L: level sensor, H: heater).

Figure 5.7 shows the design concept for the modules. The cavities are surrounded by liquid helium tanks, which are connected by "chimneys" to the two-phase supply line. The diameter of the chimneys and the two-phase line has been increased w.r.t. the standard TESLA design to be able to exhaust the fairly large CW heat load. The liquid-helium level is at 33% in the two-phase line, this being supplied by the LHe supply line via a JT-valve. The two-phase line vents to the gas return line which returns the gas to the refrigeration plant. In addition to the liquid and vapor line, there are two forward and two return lines for the 5 K and 40 K thermal shields and a cool-down/warm-up line connecting to the bottom of the cavity tanks. All vacuum insulated transfer lines that connect the refrigerator to the cold sections also contain these cold lines.

Modules 1 and 2, as well as the third-harmonic section are connected to each other in series without any warm section between them. A warm bypass around the bunch compressor then connects to the final linac module.

5.5 Layout of the Cryoplant

As seen in Figure 5.8, the cryogenic system for superfluid helium II at a temperature of 1.8 K consists of two mostly independent parts:

- A liquefier to cool helium at room temperature to liquid helium at 4.2 K (1 bara).
- A sub-cooling system to cool helium from 4.2 K to 1.8 K at a pressure of 16 mbara.

BESSY has extensive experience operating a Linde TCF50 cryoplant for BESSY II and HoBiCaT. This system is currently being upgraded with a Linde L700 plant to increase the capacity for current activities. Both plants are connected at the 4.2 K temperature level by a cryogenic line, so that the full liquefaction power can be merged in a big 10.000 l dewar. The capacity represents about 75% of that required for STARS. Taking into account helium requirements for BESSY II and HoBiCaT, STARS will be able to operate

with beam for about 12-16 hours a day with this cryoplant configuration. During operation, helium that cannot be re-liquefied will be stored in a 750-m³ gas storage. Beam time is then followed by a 12-8 h pure re-liquefaction time during the night with minimal cooling power to maintain STARS at 1.8 K.

The sub-cooling system consists of a heat exchanger cooling down the helium from a temperature of 4.2 K to 2.2 K, but still at atmospheric pressure. A Joule-Thompson valve in the feed cap to the first cryomodule expands this helium and controls the level in the two-phase line. The helium bath of the cavities is pumped to a pressure of 16 mbara corresponding to a temperature of 1.8 K. The first segment consists of a three-stage cold-compressor system operating below 20 K. The gas then flows through a heat exchanger connected to the liquefier L700 which warms up the gas to room temperature and increasees the liquefaction rate of the liquefier. A set of four parallel vacuum pumps will compress the gas to atmospheric pressure. This gas is fed to the compressors of the liquefiers.

Shield cooling of the modules is provided by 4.2 K helium. Both the 4/8 K and the 80 K shields are connected in series. The cold return gas is fed back to the liquefier L700 to increase the liquefaction rate und to warm up the gas to room temperature.

The overall layout of the cryogenic system for operation of BESSY II, HoBiCaT and STARS is shown in Figure 5.8.

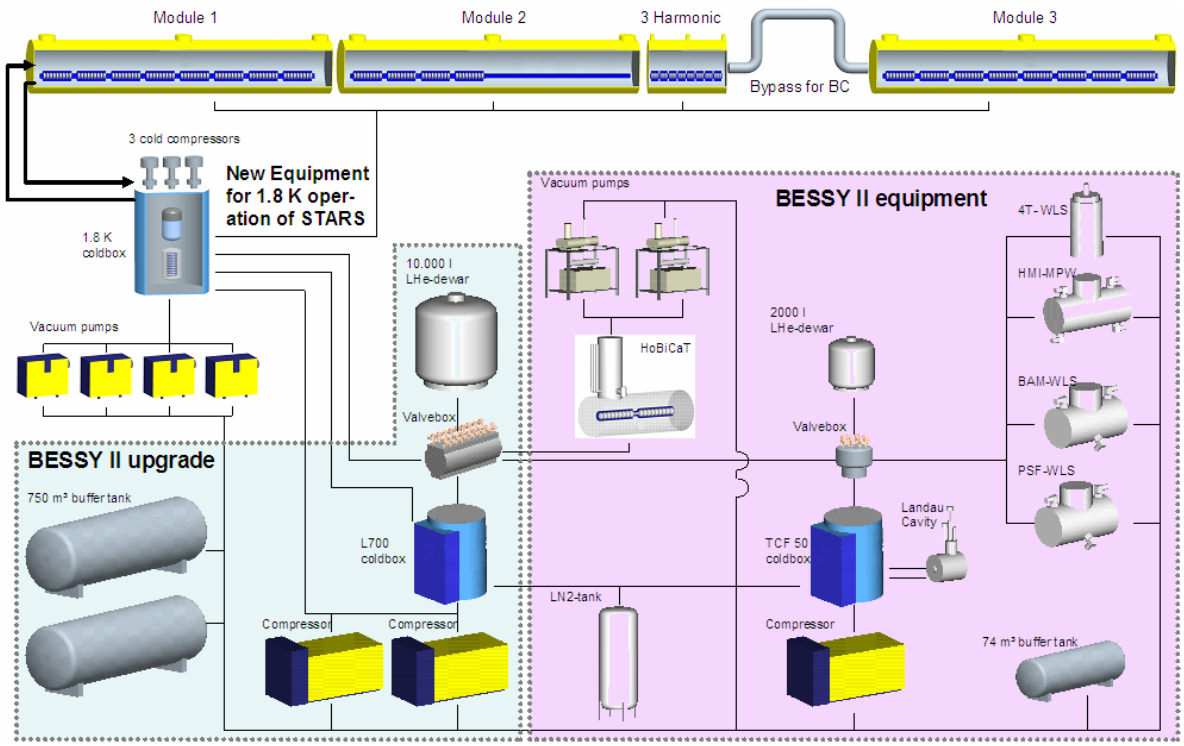

Figure 5.8: The cryogenic system of BESSY II and the STARS linac

6 Bunch Compression and Beam Tailoring

To operate free-electron lasers, high brilliance electron beams are required with high peak current, e.g. high electron density with a low transverse emittance and a small energy spread. The requirements on the electron beam quality increase with increasing FEL photon output energy. For STARS the beam parameters are listed in Table 6.1. Present-day electron source technology is able to deliver these high brilliance beams, albeit at peak currents lower than that required for efficient lasing. A magnetic chicane (bunch compressor) is therefore needed to compress the beam to high current at an energy where space charge effects no longer impact the beam quality. Clearly, the beam transport of the linac must therefore be carefully laid out to ensure that the beam quality is preserved right up to the HGHG cascade. To that end, the complete STARS facility has been analyzed, whereby ASTRA was used for the early part of the machine (gun + first module) to account for space charge effects, ELEGANT for the bunch compressor and remaining linac and finally GENESIS for the HGHG cascade.

Table 6.1: Beam parameters for STARS

Parameter	Target Value	Unit
Energy	325	MeV
Transverse emittance (sliced)	1.5	π mrad mm
Peak current	> 500	A
Bunch charge	1.0	nC
Energy spread (sliced)	0.01	%

Bunch compression is performed with a two step procedure, making use of the fact that the energy spread of the bunch is very small so that the bunch length can be reduced at its costs. First a linear correlation between the energy and the longitudinal position within the bunch is imprinted on the beam. This chirp is generated by an off-crest passage of the accelerating cavities. Then, the bunch passes a magnetic chicane, where the path length depends on the electron energy. Provided that the electrons in the head have a lower energy than those in the bunch's tail, this leads to a bunch compression.

Although in principle quite simple, several effects must be considered carefully when designing the bunch compressor. These include:

- coherent synchrotron radiation,
- space charge,
- non-linearities in the accelerating RF potential and in the bunch compression.

Details on the design philosophy of the bunch compression system are given in the TDR, Chapter 7.

The most limiting issue for an HGHG FEL such as STARS is the last one, which always results in a very high and short current peak unsuited for seeding in the HGHG cascade because it will generate strong SASE radiation. For STARS the implementation of 3rd

harmonic cavities is therefore planned to compensate for the RF and compressor non-linearities. The harmonic module is placed between module 2 and the bunch compressor.

For STARS, a single bunch compressor at about 180 MeV will be sufficient because only a moderate compression factor of order 11 is required to achieve the full 500 A peak current. At 180 MeV, space-charge effects are sufficiently low to not disrupt the beam significantly. Figure 6.1 depicts the schematic layout of the bunch compressor (including matching and emittance measurement sections), its main parameters being listed in Table 6.2.

The linac optics are adjusted to reach optimal values of the Twiss parameters in the bunch compressor, the collimator and in the FEL line at the linac end while keeping the transverse bunch dimensions in the accelerating section at reasonably small values. Superconducting quadrupole magnets at the downstream end of each module are used as well as multiplets of normal conducting quadrupoles before and after the bunch compressor and the collimator section. Figure 6.2 shows the optical functions over the entire machine.

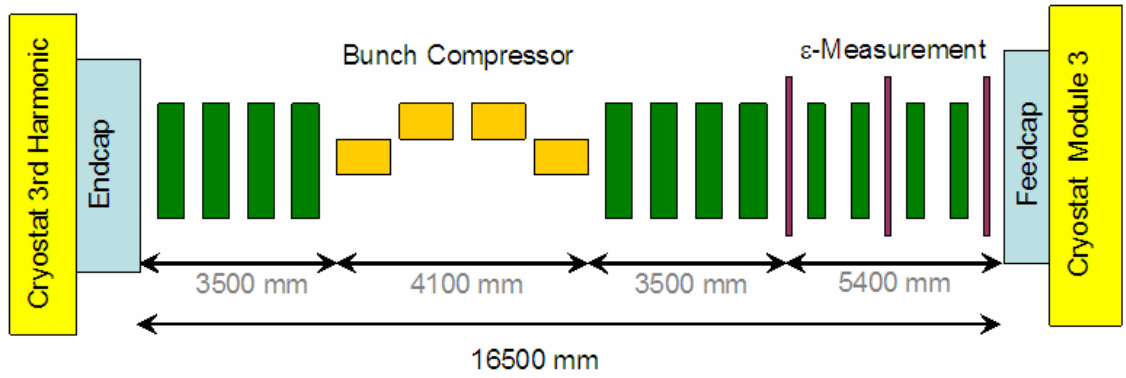

Figure 6.1: Bunch compressor and emittance measurement section. Dipole magnets are in yellow, quadrupole magnets in green.

Table 6.2: Main parameters of the bunch compressor

Parameter	Target value	Unit
Symmetric four dipole magnet chicane		
Dipole magnets:		
Length	0.4	m
Max. bending angle	20	degree
Max. magnetic field	0.51	T
R56 (reference value)	-7.8	cm
T566 (reference value)	9.8	cm
R56 @ max. bending angle	-26.9	cm
T566 @ max. bending angle	38.1	cm

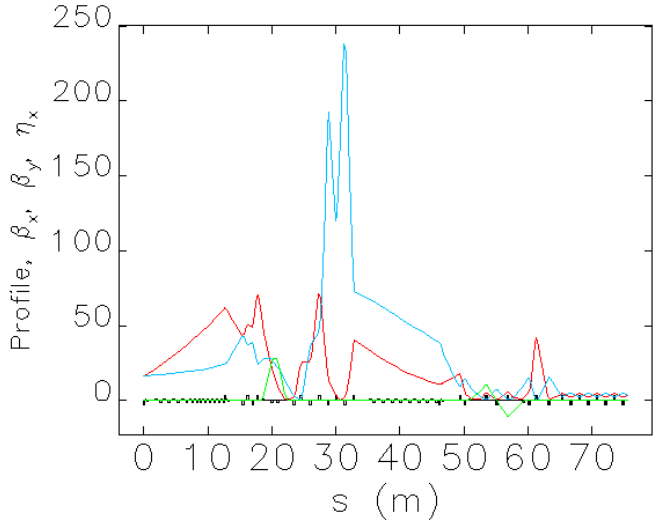

Figure 6.2: Optical functions from the end of Module 1 up to the FEL entrance.

Simulation results of the bunch distribution are shown in Figure 6.3. The peak current is increased from about 45 A at the entrance of the bunch compressor to more than 500 A at its end. The sliced emittance is conserved in both planes as well as the energy spread (apart from the increase related to the energy chirp used for the compression scheme).

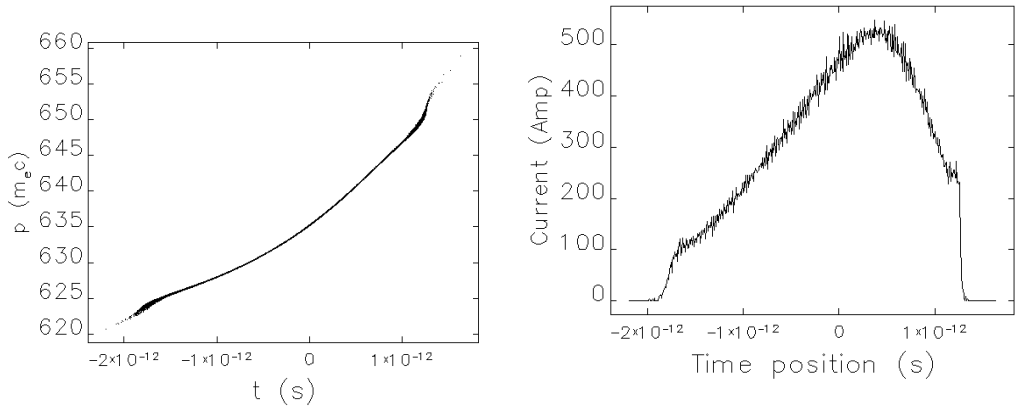

Figure 6.3: Simulated longitudinal phase space (left) and corresponding current distribution (right) of the electron bunches at the undulator entrance.

7 The HGHG Cascade

7.1 General Layout

For the BESSY FEL cascades with up to four stages will be used to seed an FEL with photon energies up to 1 keV. As a world-wide first proof-of-principle for HGHG cascading, STARS will cascade only two HGHG stages to reach a photon energy of up to 31 eV.

Figure 7.1 shows the general layout of the STARS-HGHG cascade with the main parameters listed in Table 7.1.

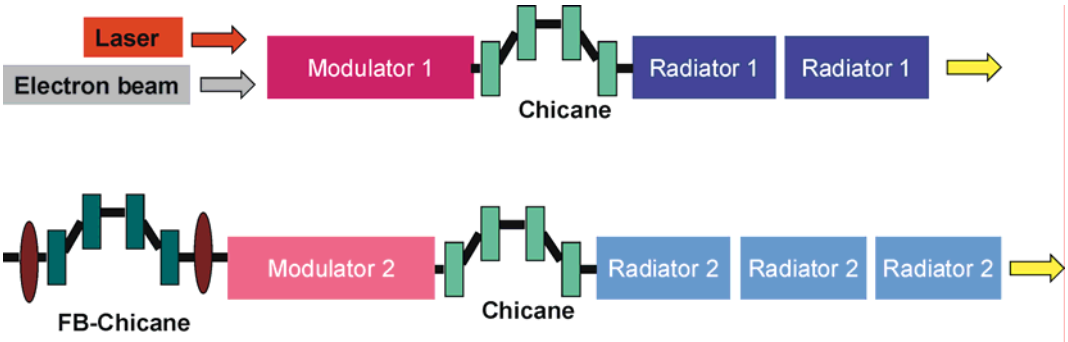

Figure 7.1: Schematic of the STARS two-stage HGHG Cascade (modulators red, radiators blue, dipole chicane green, fresh-bunch chicane dark green)

Table 7.1: Main parameters of the STARS cascading experiment

	Period length	Periods	Wavelength
MOD1	50mm	10	700-900nm
RAD1	50mm	2 x 40	140-300nm
MOD2	50mm	30	140-300nm
RAD2	22mm	3 x 150	40-70nm

7.2 Expected Performance

For predictions of the STARS performance, calculations were performed with the time-dependent 3-D-simulation code GENESIS. Details on the optimization of the HGHG process are given in Chapter 3 of the TDR.

To make meaningful predictions of the expected performance, HGHG simulations must use electron bunches obtained from complete start-to-end simulations, from the injector to the undulators. In particular, the results incorporate the impact of the energy chirp along the bunch, the non-constant current profile, and the slice-to-slice variation of the other bunch parameters. Furthermore, wake fields generated by the small vacuum chamber of the second radiator (of order 5 keV/m) were included in the calculations. Their impact proved to be negligible.

STARS will be continuously tunable from 40 nm to 70 nm, enabling proof of principle experiments throughout the whole wavelength range. This high degree of flexibility is achieved by using different harmonics (3-5) in the cascades in conjunction with gap adjustments of the undulators and variation of the seed wavelength. Full variability of the polarization is possible between 40 nm and 50 nm by using APPLE-III undulators for the second radiator.

Examples of the *linearly* polarized radiation after the first module of the final radiator are shown in Figure 7.2. Peak powers of over 100 MW (at 40 nm) and over 400 MW (at 66 nm) with pulse energies of 2.6 μJ and 11.3 μJ, respectively, are achieved. The FWHM values of the pulses are of order 20 fs, reproducing the short pulse duration of the seed laser used for the simulations. The spectral bandwidth is around 0.36% in both cases.

Even higher power levels are possible for *helically* polarized light, as shown in Figure 7.3. Here peak powers of 200 MW at 40 nm and well over 600 MW at 50 nm are achieved. The increase is due to the improved coupling between the helically polarized light and the electron motion.

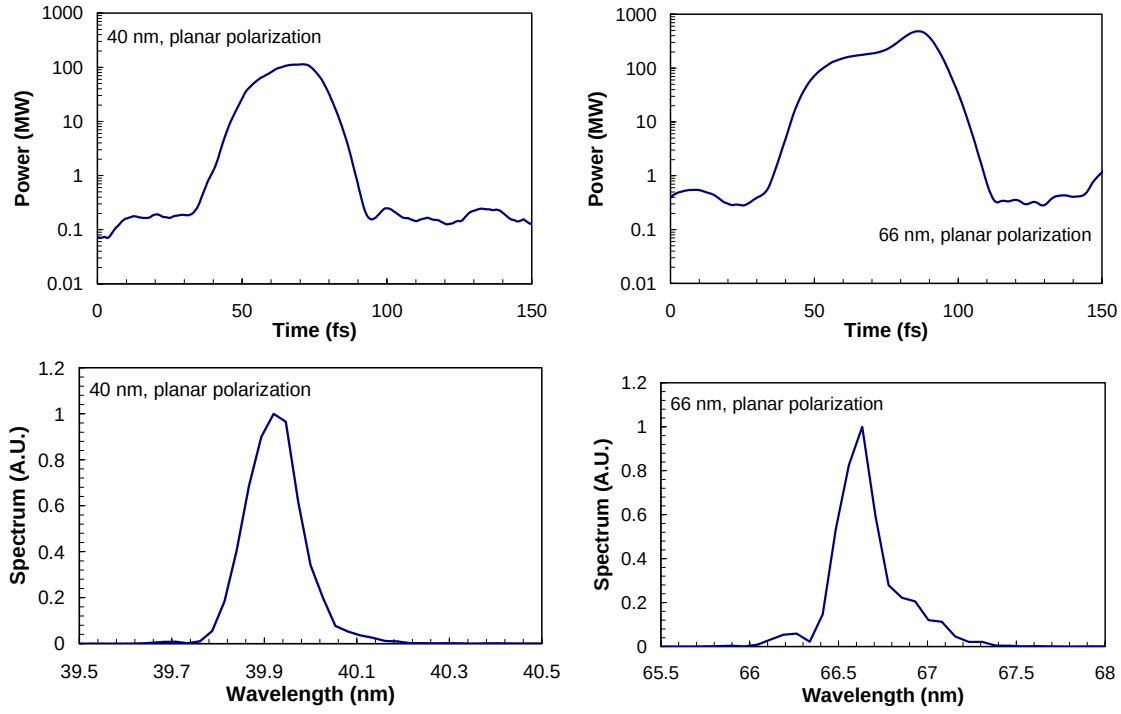

Figure 7.2: Temporal FEL pulse (top row) and spectra (bottom row) for STARS output radiation at 40 nm (left) and 66 nm (right). A comfortable signal-to-background ratio and high spectral purity is achieved.

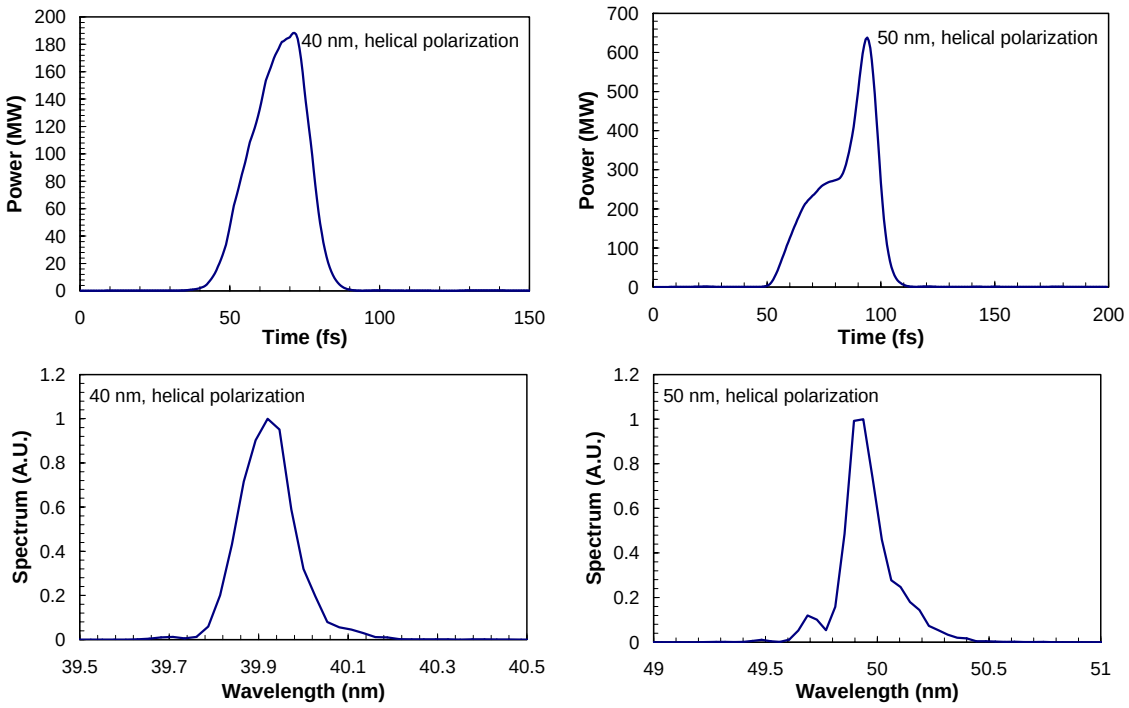

Figure 7.3: Power (top) and spectrum (bottom) after the first radiator module for the 40 nm (left) and 50 nm (right) case and helical polarization.

The second radiator is composed of 3 identical undulator modules, with individual gap control so that the radiation can be extracted at different locations along the radiator. In the above examples, the radiation is extracted at the end of the first module where a high spectral purity is achieved. However, even higher power levels can be achieved at the cost of spectral purity after additional modules. Figure 7.4 depicts the field at 50nm wavelength and helical polarization after each of the three modules. Finally, a peak power of 2.2 GW in the superradiant regime is extracted.

7.2.1 Harmonic Radiation

Wavelengths below 40 nm are also within reach of STARS by tapping into nonlinear harmonic components of the radiation field. Wavelengths down to 13 nm are accessible if the 3rd harmonic is used. An upgraded version of GENESIS 1.3 was used to study the evolution of harmonic FEL radiation in a fully time-dependant mode [13]. The recent additions to the code are based on the assumption that linear amplification is significantly smaller for higher harmonics than for the fundamental so that the non-linear interaction is the main driving force of higher harmonic bunching and coherent emission.

Figure 7.5 shows the evolution of fundamental and third harmonic radiation along the full length of the second radiator when tuned to 40 nm. The temporal power distribution at the end of the first undulator module, before the beam enters the superradiance regime, is also shown.

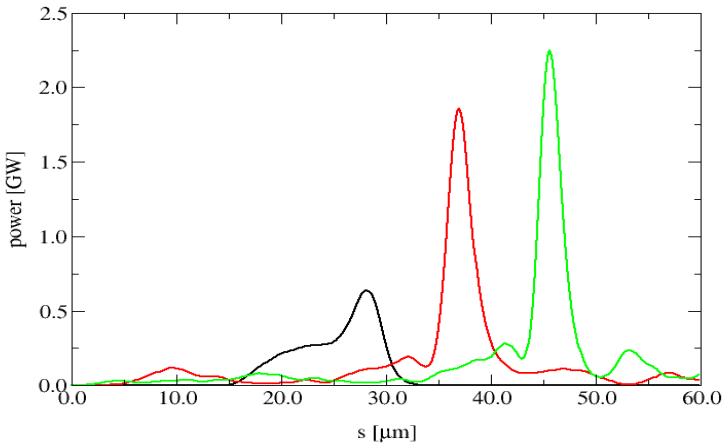

Figure 7.4: Power emitted after the first (black), second (red) and third (green) radiator module at 50nm with helical polarization. The power increases at the expense of spectral purity.

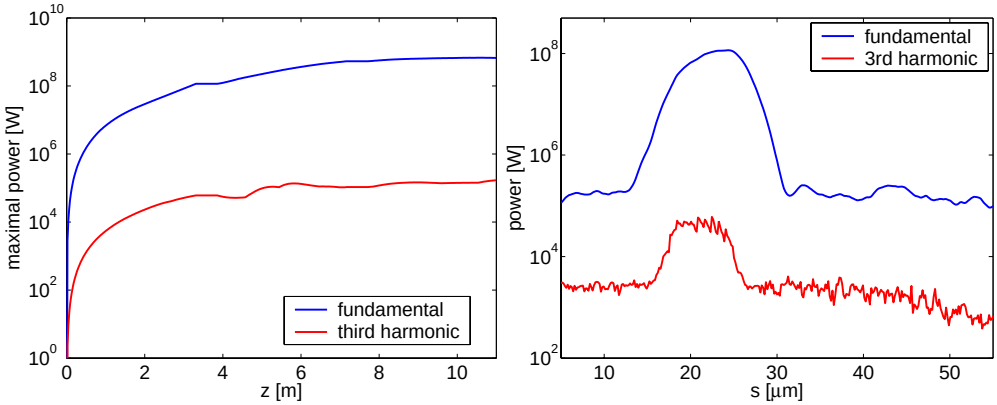

Figure 7.5: Evolution of fundamental and third harmonic radiation at 40nm and 13 nm, respectively, as observed on axis of a planar undulator. Left: peak power plotted along second radiator. Right: temporal power at the end of the first undulator module of the second radiator.

7.2.2 Operation at reduced energy

In the simulations, the HGHG cascade has been optimized for 325 MeV beam energy and a peak current of 500 A. However, STARS has been designed to be very flexible, with the option to operate at lower energy (down to 285 MeV) and lower peak current (< 200 A) while still lasing at 70 nm. Hence a staged commissioning of the HGHG cascade is possible with fewer than the full compliment of the accelerating cavities being operational and without the third-harmonic section.

7.3 Seed Laser

A Ti:Sa laser will be used to seed the first modulator at wavelengths of 800 nm for the initial proof-of-principle experiment at 67 nm. The required pulse length and energy are 35 fs and approximately 10 μJ, respectively, at 100 Hz repetition rate. These parameters are well within the specifications of commercially available Ti:Sa systems. To provide for the full STARS tuning range, a traveling-wave parametric amplifier (e.g., TOPAS®) will be added as an upgrade to the Ti:Sa laser, similar to the system detailed in the TDR. By passing the output through an SHG stage, the required seed-laser tuning range from 700-900 nm will be achieved.

BESSY has developed extensive experience operating such Ti:Sa systems for the Femtoslicing Facility in the BESSY-II storage ring [14]. Here, a femtosecond fraction of the electron bunch in the storage ring is energy-modulated in an undulator by a co-propagating fs-laser pulse. This essentially represents the first stage of the HGHG cascade for STARS.

Hence much expertise for seeding the first modulator in STARS, such as laser-beam transport, focusing, and stabilization of the longitudinal and transverse overlap with the electron bunch, already exists at BESSY. In particular, BESSY has gained much experience in the practical implementation and control of electron-laser overlap. Moreover, diagnostics to measure the energy modulation in the overlap region by means of THz radiation are in a mature state and routinely used for feedback to optimize the overlap [15] (see also Section 9.2).

To ensure a high-degree of synchronization between seed laser and electron bunch, the complete laser hutch and beam transport to the undulators will be in a climate controlled environment with a temperature stability of ±0.5 °C. Diagnostics for laser pulse length, pulse energy, wavelength, chirp and spatial profile will be included to continuously monitor and correct the laser performance.

For pump-probe experiments, a fraction of the seed laser pulse will be channeled to the experiment via an evacuated laser beamline, thereby guaranteeing an intrinsic synchronization between the pump and probe pulses. Such a setup is already operational at the BESSY Femtoslicing Facility, where a stability of better than 150 fs over 24 h has been demonstrated, the measured value currently being limited by the pulse length.

8 Undulators

Design and fabrication of world-class undulator systems is one of the most valuable assets of BESSY and many tens of meters of undulators have been produced and installed in the BESSY-II storage ring. Details of undulator design for the BESSY FEL are documented in Chapter 9 of the TDR. These can be applied directly to STARS.

The test FEL will consist of two HGHG stages with a modulator and a radiator for each stage. The first and second radiators are segmented into two and three modules, respectively. The parameters of the undulators are listed in Table 8.1.

Table 8.1: Parameters of the undulators for STARS.

Device	Total length / m	Period / mm	Design	Min. gap / mm	Max. field / T
Modulator 1	0.5	50	Planar	10	1.090
Radiator 1	2 x 2	50	Planar	20	0.589
Modulator 2	1.5	50	Planar	20	0.589
Radiator 2	3 x 3.3	22	APPLE III	7† / 4.4‡	B-hor = 0.621 B-vert = 0.839

†Physical aperture (= maximum outer diameter of the vacuum chamber).
‡Vertical gap, which determines the magnetic field strength on axis.

8.1 Magnet Structure

Various undulator technologies are discussed in the TDR of the BESSY FEL. Although some progress has been made with superconducting undulators, the phase errors are still too large and the Fe-dominated structures show hysteresis effects which are not acceptable for FEL applications such as STARS. Hence, permanent magnet technology will be used for STARS. Many planar, in-vacuum devices have been installed in third generation machines, but so far none have been built for variable polarization. Therefore, out of vacuum undulators have been selected for STARS.

Modulator 1, Radiator 1 and Modulator 2 are all planar devices. Although helical devices would reduce the overall length of the modules, the cost for these would be unnecessarily high. Only Radiator 2 needs to be helical to provide full polarization control of the output radiation. As seen in Table 8.1, Modulator 1 requires the highest field necessitating a minimum gap of 10mm and a magnet block height of 40 mm. For Radiator 1 and Modulator 2 a minimum gap of 20 mm is sufficient using the same magnet blocks.

The last radiator (3 modules) will be realized as an APPLE-III device providing full polarization control of the radiation. The free aperture for the vacuum pipe between the magnets is 7mm and the smallest vertical distance is 4.4 mm which provides enough

space for Hall-probe measurements as well as for a fixture to support the vacuum chamber. An APPLE-III type structure has been chosen for a number of reasons:

- For the same minimum aperture (7 mm in this case) the APPLE-III device provides a factor of 1.35 higher fields when compared to the APPLE-II design.
- The natural focusing of an APPLE-III design is smaller than that of an APPLE II.
- The APPLE III design provides space for the installation of glass fiber radiation monitors (to detect beam loss) close to the electron beam without sacrificing gap (the diameter of Cherenkov glass fibers is 0.7 mm).

Although it is true that APPLE-II devices can achieve the same fields as the APPLE III by using smaller gaps, the beam-pipe aperture becomes unacceptably small, complicating the undulator alignment and design of the up-stream collimator.

The field optimization of APPLE-II devices has been described in [16]. An APPLE-III prototype structure will be built to adapt the shimming techniques to the new design.

8.2 Support and Drive System

In the following we briefly review the basic features of the support and drive system. More details can be found in the TDR and in [17].

The gap and phase motion are realized with servo motors operating in feedback mode with absolute encoders. The gap is measured directly above the electron beam thereby avoiding Abbe's comparator error. A gap reproducibility of 1 μm has been demonstrated for such a system at BESSY. The temperature dependent gap error is only 1.1 μm/°C which is negligible when compared to the thermal variation of the magnet material remanence. Climate control in the undulator region will be implemented to maintain a constant temperature to within ±0.5 °C.

The magnets are mounted into Al-keepers assembled onto Al-girders. It has been demonstrated that 4-m long girders can be fabricated with a flatness of ±8 μm [17]. Remaining gap errors can be compensated with mechanical spacers. The bending of the long girders is minimized with four supports instead of two using two crossbars inside the magnet girders. The bearings are constructed such that tapering is possible.

The support structure of Radiator 2 is made from a single piece of cast iron. This provides a very stiff structure that can cope with the strong APPLE 3D forces and a bionic optimization of the structure can easily be applied [17].

The supports of the other undulators can be welded structures as well because only vertical forces are present.

8.3 Vacuum Chamber

In Radiator 2, the inner diameter of the vacuum chamber is 5 mm. An analysis of the wakefields was performed to estimate their impact on the FEL performance. The dominant sources were found to be the resistive wall wakes and the effect of geometry at the diagnostic ports, each contributing about 50% to the total wakefield. Maximum calculated values were of order 5 kV/m. These were included in the GENESIS simulations of the HGHG cascade and found to have no impact. A comparison with published LCLS wakefield calculations [18] is also favorable because the peak current in STARS is more than 20 times smaller.

Given 3-m long modules for Radiator 2 with pumping between modules, the expected vacuum profile was also determined. Peak pressures are expected to be at worst in the 10^{-6} mbar range. Measurements with commercially available tubing and an inner diameter of 4 mm yielded even lower values, of order 5×10^{-7} mbar. Gas pressures in this range are not expected to produce significant radiation damage in the undulators or impact the photon flux. GEANT calculations performed for the FEL vacuum pipe verified this statement [19].

8.4 Undulator Operation

The natural focusing depends on the transverse field profiles which changes with gap and row phase of the variably polarizing Radiator 2. The focusing strength has an impact on the electron-beam size [17] and has to be compensated to optimize the FEL process. In an FEL the beam size is symmetrical in both planes and iron shims cannot be used. Hence an active compensation scheme has to be adopted. The Radiators 1 and 2 are split into two and three modules, respectively, and the phase has to be adjusted between these modules. Permanent magnet phase shifters will be used for this purpose in order to avoid hysteresis effects.

9 Beam Diagnostics & Timing Distribution

9.1 Diagnostics in the Main Linac

Clearly, the beam parameters must be observed and controlled along the entire length of the linac and in the undulators with high precision to guarantee optimum performance of STARS.

The main function of electron diagnostics is

- to enable the commissioning of the accelerator,
- to verify and control the quality of the electron beam for efficient lasing, and
- for machine protection.

Figure 9.1 and Figure 9.2 depict the distribution of the major diagnostic components in the gun section and along the linac. Redundancy was folded into the layout to improve the reliability of the diagnostics. Provided here is only an overview of the main components to be used, with details of all the techniques being given in the BESSY-FEL TDR.

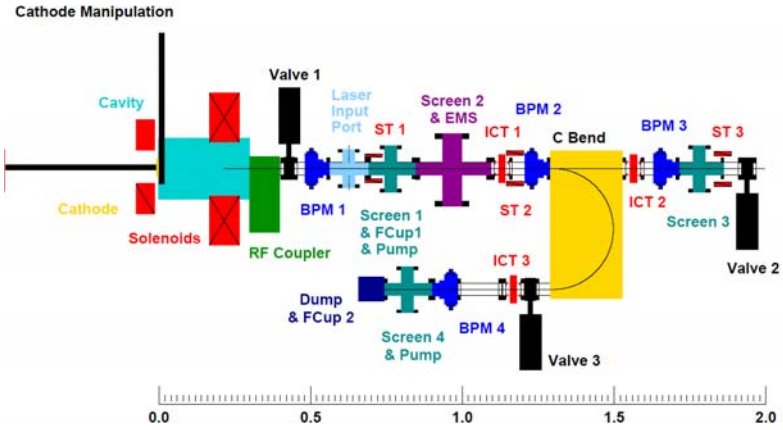

Figure 9.1 Layout of the injector diagnostics up to the entrance of the first accelerating module.

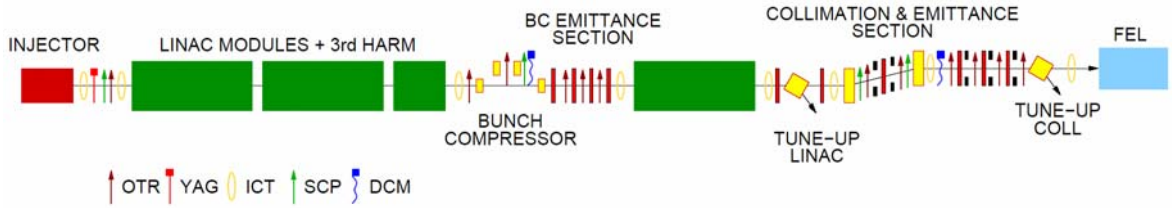

Figure 9.2: Distribution of linac diagnostic components: Optical transition radiation stations (OTR), viewscreens (YAG), integrating current transformer (ICT), streak camera ports (SCP), and diffraction compression monitors (DCM).

Key diagnostics include the emittance measurement sections after the bunch compressor and directly in front of the undulators. Thus it is possible to commission all key components of the linac in sequence and characterize the beam before injecting into the subsequent section.

First the injector will be commissioned with emittance measurements at low energy. The beam is then transported through the first linac including the switched-off bunch compressor and on to the linac tune-up dump. Thereby an emittance measurement at high energy without space-charge effects is possible prior to commissioning the compressor. The same setup then is used to characterize the beam during the commissioning of the bunch compressor. Finally, the beam is injected into the collimation dogleg through the second emittance-measurement section and into a further tune-up dump to safely commission the entire linac up to the FEL entrance. Only when this is completed, will the beam be injected into the FEL.

Since the photon beam properties are directly linked to the electron beam parameters, it is essential to map the six-dimensional phase space at the entrance of the undulators. For machine protection, crucial beam parameters, such as charge and position, have to be observed on a bunch-to-bunch basis. Fast stripline BPMs with digital readout electronics will enable single-shot measurements of the beam trajectory. Integrated current transformers and Cherenkov radiation detectors based on fiber optics will monitor beam loss.

9.2 Diagnostics in the HGHG Cascade

Inside the undulator sections, special radiation and electron trajectory diagnostics are necessary to monitor the FEL process. In particular, it is crucial to establish proper overlap between seed laser radiation and electron beam and subsequently between the amplified radiation pulse and the electron beam.

The general layout of the diagnostics in the undulator section is depicted in Figure 9.3. Details of each of the components are given in Chapter 12 of the TDR.

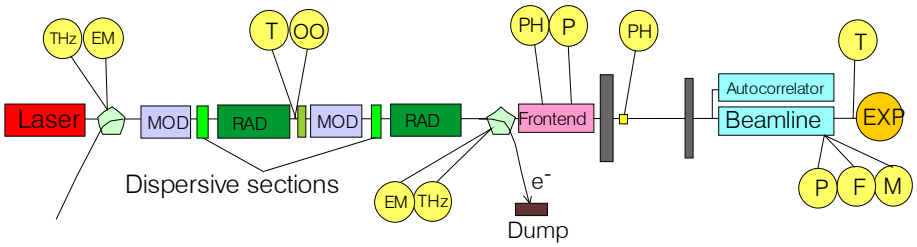

Figure 9.3: Overview of diagnostics proposed for the HGHG cascade. THz diagnostics (THz), emittance monitors (EM-SR), timing diagnostics (T), optical overlap (OO), pinholes and intensity monitors (PH), position diagnostics (P), flux monitors (F), microfocus detection (M).

One of the key parameters of the HGHG process is the laser interaction with the bunch within the first modulator, where the overlap between the seed laser and electron bunch is critical. BESSY has gained valuable experience at the BESSY-II Femtoslicing facility [14], [15] where a number of systems are now in routine operation to optimize this overlap (see Chapter 12 of the TDR and [20]).

Transverse overlap of the seed laser and electron beam, as well as coarse timing on the 10 ps scale, is achieved by imaging the seed laser and spontaneous radiation in the Modulator with a telescope (NIR and visible light). The off-axis modulator radiation is red shifted so that it is easily differentiated from the seed laser. Relative timing information between the two signals is measured with an avalanche photodiode and thus can be used to adjust the overlap down to a few ps.

Fine tuning of the overlap is then achieved by observing the THz radiation emitted by the 35-fs slice of the bunch that has interacted with the seed laser. For this, a THz beamline, as currently employed at BESSY II [21], will be used. Following the dispersive chicane, this is translated into a density modulation which radiates in the far-infrared. The signal scales quadratically with the electrons in the slice so that optimal overlap can readily be determined. By changing the phase between laser and bunch, the bunch profile can be measured as well (see Chapter 12 of the TDR). THz radiation from the full bunch can furthermore be used to determine the beam shape [22],[23] and to image the beam [24].

This technique is extremely powerful because there are no other background sources in the far infrared which can interfere with the measurement. Measurements performed at the Femtoslicing facility at BESSY II in the low-alpha mode amply underscore this statement (Figure 9.4). Here the bunch spectrum can easily be separated from the spectrum generated by the fs-slice that interacted with the laser. As a result, the dynamic range of the THz diagnostics is extremely large. An example making use of this fact is given in Figure 9.5, where the resonance between seed laser and undulator was detected by means of the THz signal. A dynamic range of 4 orders of magnitude could easily be measured yielding useful information even when the undulator is detuned by many bandwidths from the resonance [25]. The side bands are caused by the fact that the undulator has a finite number of periods (10).

9.3 Timing Distribution

Nearly every component of STARS will require precise timing signals for synchronization. This includes the photocathode and seed lasers, the entire RF system, and of course, the diagnostics. Moreover, to exploit the ultra-short pulses, the experiment at the FEL output has to be synchronized to the same accuracy. With optical pulses on the order of tens of femtoseconds and RF stability requirements of order 0.05-0.1 deg, the timing system has to be significantly more accurate than 1 ps. This appears to be beyond

the capability of conventional RF distribution systems based on temperature stabilized coaxial cables.

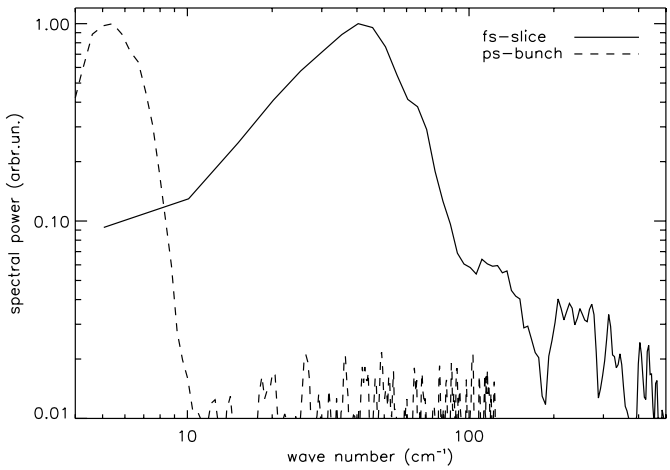

Figure 9.4: THz spectra of a 1.2 ps (RMS) long bunch and from a laser-induced density modulation caused by femtosclicing in the BESSY-II storage ring. A high-pass filter can easily remove the background radiation from the ps-bunches.

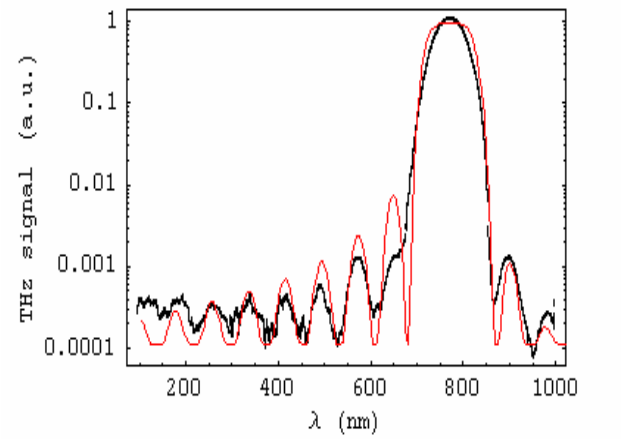

Figure 9.5: Detection of the FEL resonance in the modulator (U139) of the BESSY-II femtoslicing facility. The THz signal due to the bunch-laser interaction was measured as a function of undulator gap, thereby shifting the resonant wavelength of the undulator according to Equation (1). The signal is maximized when the laser is in resonance with the undulator. Measured values are given by the black curve. Theoretical calculations are shown in red.

Rather, a very promising alternative based on optical means will be employed. This system uses an optical fiber oscillator as a Master Oscillator (MO) and the signal distribution is performed via stabilized fiber links [26].

An Erbium-doped optical fiber laser inherently has little phase noise, especially at higher frequencies (> 10 kHz). At lower frequencies the laser suffers from more phase noise due to microphonics and thermal drifts. On the other hand, a microwave oscillator exhibits very little phase noise at low frequencies. By synchronizing the fiber laser to a microwave oscillator in the low-frequency range thereby provides a very low noise master oscillator.

Since optical pulses are not sensitive to electric and electromagnetic noise, distribution by optical means has inherent advantages over an RF distribution via coaxial cables. Nevertheless, with a temperature dependent refractive index on the order of 10^{-6} /°C length stabilization by, for example, piezo stretchers must be implemented. In a test at MIT in an accelerator environment, such a stabilized distribution system of 500 m length only produced an additional jitter of 12 fs [27].

The extraction of an RF-signal from the optical information by direct conversion using photodiodes is limited by excess phase noise that stems mainly from amplitude-to-phase conversion in the photodetection process. This problem is overcome by a balanced optical phase detector [28]. With such a system, the jitter in the conversion process could be reduced to only 3 fs.

For synchronizaton between two optical sources a technique called balanced optical cross-correlator can be applied. This scheme was successfully tested in synchronizing a fs Cr:Fo and Ti:Sa lasers to fs accuracy [29]. This scheme may be adapted to also synchronize the photocathode (ps) and the seed (fs) laser.

9.4 Beamline

The beamline is the interface between the FEL and user experiment. It serves not only as a transport system for the photon beam from the end of the FEL to the users experiment, but tailors the radiation in terms of bandwidth, pulse length and photon density. BESSY has the full expertise required for beamline design, having developed more than 40 beamlines for BESSY II.

A detailed description of the FEL-specific requirements, as they also apply to STARS, is given in the TDR for the BESSY FEL, Chapter 10. STARS will be equipped with a monochromatic and a white light beamline that operate alternatively. The selection between both is made by switching the first mirror.

A collimated plane-grating monochromator is used to deliver monochromatic light of a defined wavelength, whereas the white light beamline focuses the beam as strongly as possible. The conceptual design of the monochromatic beamline, as shown schematically

in Figure 9.6, illustrates that even with limited space the full flexibility of this kind of monochromator can be obtained.

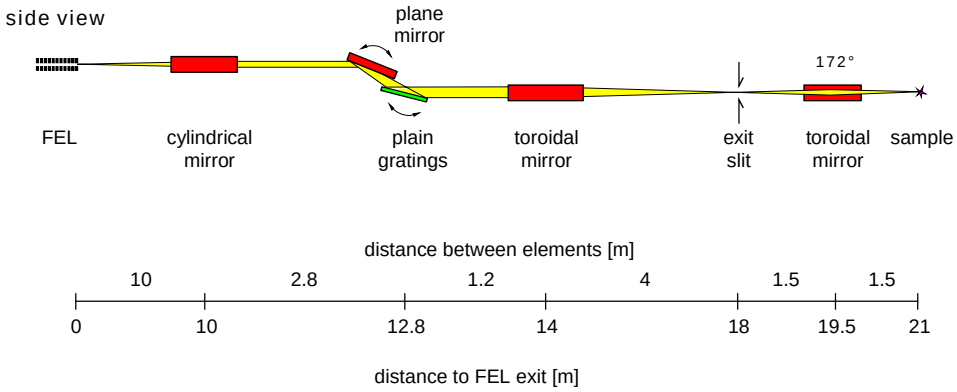

Figure 9.6: Monochromatic beamline for STARS.

9.5 Photon-Beam Diagnostics

Finally the characterization of the FEL beam (e.g., pulse energy and profile, lateral position, spectral content of the pulses, the temporal profile) must be performed to benchmark the simulations.

Flux monitors based on gas detectors are an integral part of the monochromator design at the BESSY-II beamlines. They are used to measure the relative spectral flux and determine the spectral resolution. In STARS, absolute photon flux and pulse energy will be determined with gas detectors developed by the Physikalisch-Technische-Bundesanstalt (PTB) at BESSY [30]. This detector is based on an ion counter, where the photon pulse is passed through a rare-gas cell. Pulse-to-pulse measurements are possible, and a very high dynamic range can be covered by adjusting the gas pressure and the electronic sensitivity of the detector. Their operation has been proven at FLASH and SPPS.

Given the absolute spectral flux and energy resolution, the absolute brilliance of the FEL pulse can be determined by measuring the size and position of the final focus. This is done with conventional X-Ray-CCD focus detection. Furthermore, single-shot spectra will be measured at STARS with an open exit slit of the monochromator and fast-detector arrays, as currently under development for the BESSY Femtoslicing Facility. Since BESSY 11II provides beamlines for the same wavelength range as STARS, calibration of this equipment can take place before STARS is operational.

Non-linear autocorrelation will be used to measure the temporal structure of the FEL pulse. Here the pulse is split into two pulses by means of a geometrical beam splitter.

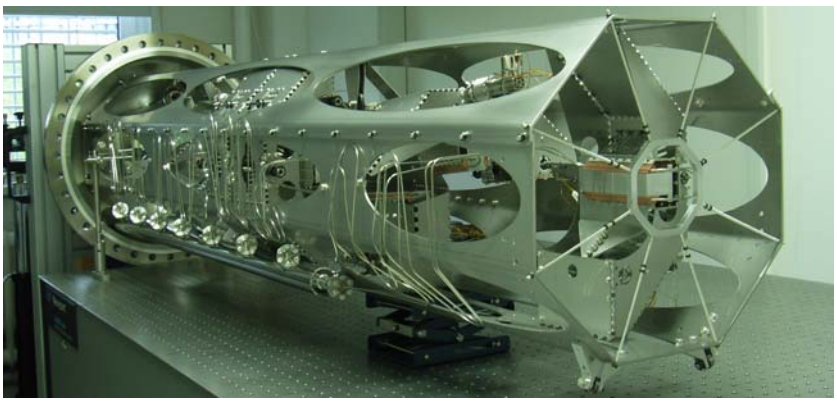

Figure 9.7: Photograph of the beam splitter and delay unit during mechanical tests.

These are passed through an adjustable delay (up to 20 ps) and subsequently merged again behind the unit. A prototype of such a beamsplitter and delay unit for the VUV has been constructed for FLASH by BESSY [31] (Figure 9.7). Assembly and testing of this instrument is currently under way, with operation in FLASH starting in 2007.

For nonlinear detection of the recombined pulses, two-photon photo emission and two-photon double ionization of rare gases are the processes of choice to unambiguously obtain pulse-shape information with fs resolution.

Cross-correlation of the FEL pulse with an ultra-short optical laser pulse (such as the seed laser) can also be applied for additional redundancy in the profile measurement. The time-delayed FEL beam is passed through a gas-phase (magnetic bottle) electron spectrometer. Part of the seed laser pulse is also deflected into the volume of this spectrometer. Given a temporal and spatial overlap of the two pulses, additional sidebands, spaced by the seed-laser photon energy, are observed in the photoemission spectrum. For rare gases, the emission spectrum is quite discrete and very well known, making the new side bands easily detectable. By adjusting the time delay the temporal shape of the FEL pulse is recorded. This scheme has been installed and tested at BESSY using a high-harmonic-generation (HHG) laser-source in the same photon energy range to be covered by STARS.

As is, this scheme does not yield shot-to-shot profile measurements. As an extension, though, an imaging spectrometer is being designed which makes use of the same physical process. Imaging the electron source onto a two-dimensional detector both a spatially and energy-resolved image of the electron source is obtained, thereby providing profiles of each individual pulse.

10 Evaluating Experiments

The experiments planned for STARS are designed to demonstrate the scientific capabilities of an HGHG-FEL source. Specifically, the experiments address applications that require the coherence and the controlled, reproducible pulse shape of such a source. Hence, for the direct FEL beam the demonstration experiment covers the general area of time resolved (coherent) imaging, whereas the monochromatized beam will be used to demonstrate STARS' time resolved spectroscopy capabilities. The experimental facilities will be constructed in a flexible fashion to enable a program involving external users once the initial characterization of the FEL output has been performed and the capabilities of such a second generation FEL have been successfully demonstrated.

A major advantage of FEL sources over existing storage ring based sources is the availability of a tremendously increased number of photons per coherence volume in connection with the availability of controlled, reproducible femtosecond pulses of soft x rays. The proposed experiments take advantage of these key FEL properties. As discussed below, the intrinsic synchronization in an HGHG FEL between the FEL pulse and the seed laser is another feature that is critical for pump-probe experiments.

Clearly, the resulting methodology being developed at STARS will have a big impact, enabling future FEL users to utilize these key properties for x-ray experiments in their own scientific area, which will certainly extend beyond solid-state physics.

10.1 Direct Beam: Imaging Experiments

The aim of the proposed experiment is to demonstrate the capability of an HGHG FEL source in performing time-resolved stroboscopic imaging experiments. Here, two femtosecond x-ray pulses hit a sample in close succession, with a well controlled time delay between the two pulses, ranging from a few femtoseconds up to 25 picoseconds. Information on the structural evolution of the sample during the time interval can be obtained (a) in reciprocal space by analysis of the coherent diffraction pattern or (b) in real space by imaging the sample structure. The goal of the experiment is to implement both techniques, perform demonstration experiments and to study the advantages and drawbacks of the two approaches. Also, the extendibility of these concepts to significantly shorter wavelengths for future work at the BESSY FEL and XFEL shall be evaluated.

The development of time-resolved scattering techniques at FEL sources will enable a variety of scientific opportunities in various areas, because it makes the femtosecond-nanometer region available to element-specific x-ray experiments. Future opportunities in solid-state physics are studies in the areas of magnetic and lattice excitations, dynamics of glasses and liquids, excitations in Bose-Einstein condensates and critical fluctuations.

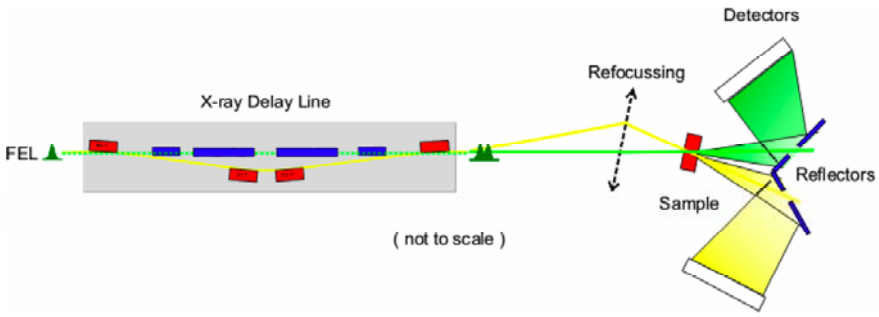

Figure 10.1: Optical layout of the time-resolved imaging experiment in the angular separation mode.

Also, these techniques enable the study of the formation and breaking of chemical bonds in processes such as protein folding and in general the dynamics of macromolecules. This would ultimately establish single macromolecule imaging capabilities at FELs, to solve protein structures for non-crystallizable proteins or enzymes.

We propose to make first steps in this direction by the following approach: Two time delayed x-ray pulses are created using the setup described in Section 9.5, in particular Figure 9.7. By a refocusing mirror, the two x-ray pulses are brought to spatial overlap on the sample, and the speckle pattern due to coherent diffraction of the x-ray pulses by the sample is recorded. Given the measurements by H. Chapman et al. at FLASH [32], where 60 nm spatial resolution could be achieved using soft x-rays of 32 nm wavelength, we expect to achieve a comparable resolution at STARS.

Two different methods, as depicted in Figure 10.1 , will be investigated.

1. *Collinear Modus*: The two x-ray pulses are quasi-parallel (< 2 mrad angular separation) and create coherent diffraction patterns on the same 2D detector. The sample dynamics can be inferred from the changes in the speckle pattern generated by the individual pulses. The diffracted light from both pulses is added incoherently at the detector by reading out the frame after both pulses have arrived. Hence, the contrast of the measured interference pattern is reduced if the sample structure changes during the delay time. The advantage of this technique is that scattering to high angles can be easily recorded yielding high spatial (and temporal) resolution and the detector read-out time is not critical. However, no real space image of the sample can be obtained and any beam-position variation at the entrance to the x-ray delay line influences the contrast at the detector.
2. *Angular Separation Modus*: The two x-ray pulses are incident on the sample under at an angle (>50 mrad), generated by stronger refocusing. As a result, the coherent diffraction patterns can be recorded on two separate detectors. If the sample is designed accordingly, real space images corresponding to the two arrival times of the x-ray pulses can be obtained by x-ray holography or iterative phasing of the

oversampled diffraction pattern. Hence, real space images at each point in time are accessible, giving access to all spatio-temporal correlations within the momentum transfer and beam delay intervals.

10.2 Monochromatized Beam: Spectroscopy Experiments

Time resolved fs electron spectroscopy reveals the dynamic response of the electronic system to an external stimulation. This could be the response of a system to a laser pulse, such as magnetic data storage material in magneto-optical recording, the dynamics of the charge carriers in a photoconductor or solar cell, or the start of a photochemical reaction. For the study of the equilibrium state, photoemission spectroscopy has been developed as an indispensable tool to characterize the electronic properties or the functionality of all these systems or devices. The extension of these studies to the time domain appears straightforward, but is currently hampered by the availability of controlled fs photon pulses of sufficiently high energy to perform photoelectron spectroscopy of the entire valence band and core levels. STARS will provide exactly the pulses needed for such studies. Especially the intrinsic synchronization between the seed laser and the FEL pulse is a critical prerequisite. Furthermore, since the intrinsic time scale of the electronic relaxation phenomena is on the order of a few fs, pulses in the fs range are also required. STARS is able to provide such pulses, and the entire valence band of solids can be reached sprectroscopically. With the use of the higher harmonics (see Section 7.2.1) even shallow core levels can be studied.

The experiments require a monochromatized fs VUV/soft x-ray source and a synchronized external laser pulse. The latter is provided by the seed laser. Samples will initially be solid films or single crystals, or samples in the gas phase. At a later date, the study can be expanded to liquid jets.

Experiments at the STARS beamline will make use of both the fundamental and harmonics of the FEL radiation. This beamline will be equipped with an endstation containing a cryogenically cooled manipulator, a sample preparation and transfer system, and a commercially available, high-resolution, high-transmission electron spectrometer. Alternately a gas-phase sample cell will be used in this setup.

11 Conventional Facilities

The STARS building and infrastructure will be developed in close co-operation with the Max-Planck-Gesellschaft. For this reason a contract ("Geschäftsbesorgungsvertrag") was already signed in August 2006.

11.1 General Concept and Layout

Figure 3.2 depicts the location of the STARS facility on the BESSY site in Berlin-Adlershof. This is the same site as planned for the BESSY FEL and hence all geological and ground stability analyses described in the TDR, Chapter 15, apply to STARS as well. The location was chosen for three main reasons:

1. It is as close as possible to the existing cryogenic installation for BESSY II/HoBiCaT, thereby minimizing the length of an otherwise costly cryogenic supply line to STARS.
2. STARS will be located immediately adjacent to the existing Schwerlasthalle. This can thus be used to house components such as the RF transmitters, thereby reducing the size and cost of the new STARS building.
3. At the proposed location, STARS will not interfere with the planned BESSY FEL and thus can continue operation even after construction of the BESSY FEL.

The layout of the STARS building is shown in Figure 11.1. The main accelerator facility will be housed in a building approximately 140 m long and 10.5 m wide. Additional enclosures within the main building are adapted to specific needs and provide local environmental control. For example, laser rooms require temperature control at the 0.5 ºC level as well as humidity control, whereas the main linac requires radiation shielding. This "house-in-house" concept provides a very cost-effective solution but still maintains the flexibility needed for a research facility.

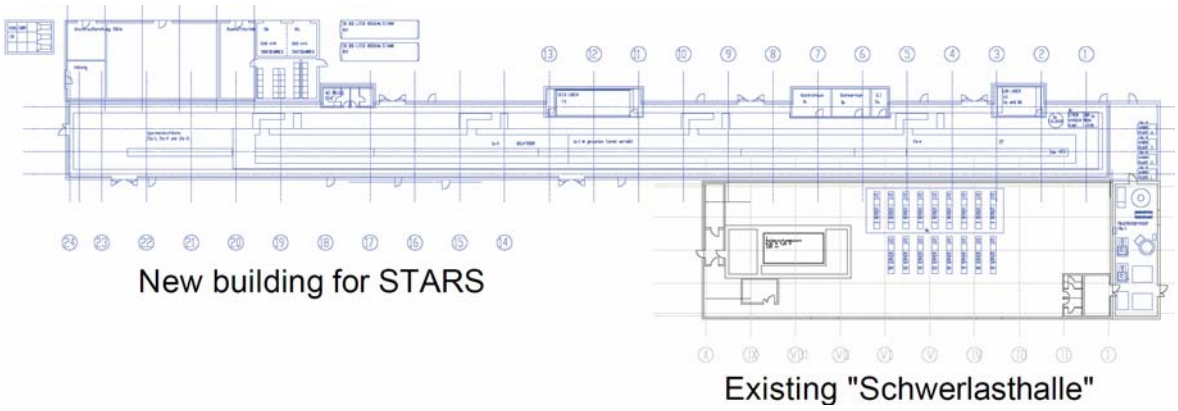

Figure 11.1: Layout of the STARS building (blue) alongside the existing Schwerlasthalle (black). STARS infrastructure is marked in blue.

Conventional installations will be located in two add-on buildings immediately adjacent to the STARS building and the existing Schwerlasthalle. One of these already exists and houses part of the BESSY cryogenic plant.

11.2 The FEL Building

The STARS building structure is essentially the same as that of the existing Schwerlasthalle. The story-frame construction is based on I-beams for columns and girders to support the ceiling. The I-beams are founded on a concrete sleeve foundation in an unshored pit. The reinforced-concrete ground plate sits on top of this and consists of two parts: one for the building foundation (along the perimeter) and one for the accelerator area. This approach limits the vibrations transmitted to STARS.

The walls consist of a sandwich structure with expanded polystyrene insulation between metal sheeting, as used for industrial buildings. The roof will not be ventilated.

Radiation shielding is provided by prefabricated steel-reinforced heavy concrete blocks. The tunnel width is 3.8 m (inside dimension). A crane spanning the entire width of the STARS building can be used to stack and remove blocks as required. This allows one to crane the accelerating modules into position through the ceiling of the radiation enclosure, thereby reducing the required tunnel width.

11.3 Supply Installations

Wherever possible, existing infrastructures from BESSY will be used to supply STARS. Among these are the de-ionized water supply for the cooling plant, compressed air and other technical gases. Similarly, liquid helium will be supplied by the existing BESSY cryogenic plant (as discussed in Section 5.4). However, a new electrical power supply plant and a cooling installation are required.

11.3.1 Electrical Power

BESSY's existing power supply station is operating near full capacity. Therefore two new 10/0.4 kV transformers and a new switching station need to be installed. These will be supplied by existing 10 kV cables. A separated system approach will be adopted, one transformer supplying power for motors, compressors pumps etc., and the other supplying power for the IT system and other sensitive electronic components.

11.3.2 Cooling Installation

A new water cooling system is needed for heat removal. This will be installed in the technical area of the building. The heat will be transferred by a cost-efficient wet cooling tower with several cooling circuits for different water quality and temperature control requirements.

For air conditioning, critical STARS equipment will be housed in individually, locally air conditioned hutches to limit the size and cost of the air conditioning system. The main part of the linac tunnel will be equipped with simple ventilation units. Recirculation coolers will be installed where necessary.

12 References

[1] D. Krämer E. Jaeschke, W. Eberhardt, (editors), "The BESSY Soft X-Ray Free Electron Laser", Technical Design Report, ISBN 3-9809534-0-8, BESSY, Berlin, 2004.

[2] German Science Council: „Stellungnahme zu zwei Großgeräten der naturwissenschaftlichen Grundlagenforschung: Freie-Elektronen-Laser für weiche Röntgenstrahlung (BESSY FEL) und eisbrechendes Forschungsbohrschiff (AURORA BOREALIS)", Mai 2006 (Drs. 7269-06) http://www.wissenschaftsrat.de/texte/7269-06.pdf

[3] L. H. Yu et al., NIM A **318** (1992), 726

[4] M.V. Hartrott et al., "Status and First Results from the Upgraded PITZ Facility", *Proc. 27th International Free Electron Laser Conference (FEL 2005)*, Stanford, California (2005), 564-567.

[5] B.E. Carlston, "New photoelectric injector design for the Los Alamos National Laboratory XUV FEL accelerator", *Nucl. Intr. Methods Phys. Research* A285 (1989) 313-319.

[6] L. Serafini, J. B. Rosenzweig, "Envelope analysis of intense relativistic quasilaminar beams in RF photoinjectors: A Theory of emittance compensation.", *Phys. Rev. E*, Vol. **55** No. 6 (1997), 7565-7590.

[7] F. Marhauser, "High power tests of a high duty cycle, high repetition rate RF photoinjector gun for the BESSY FEL", *Proc. of the 2006 European Particle Acceletator Conference*, Edinburgh, Scotland (2006), 68-70.

[8] F. Stephan et al. "Recent Results and Perspectives of the Low Emittance Photoinjector at PITZ", *Proceedings of the FEL 2004*.

[9] I. Will, Max-Born-Institute, private communication.

[10] E. Harms, H. Edwards, T. Arkan, H. Carter, C. Cooper, M. Foley, T. Khabiboulline, D. Mitchell, D. Olis, A. Rowe, N. Solyak, S. Tariq, "Status of 3.9-GHz Superconducting RF Cavity Technology at Fermilab", *Proc. 2006 Linear Accelerator Conference*, Knoxville TN, USA, 2006.

[11] J. Knobloch et al., "CW operation of the TTF-III coupler", *Proc. Proceedings of the PAC 2005*.

[12] A. Neumann et al., "Characterization of a Piezo-based microphonics compensation system at HoBiCaT", *Proc. Proceedings of the EPAC 2006*.

[13] Kathrin Goldammer, BESSY, private communication

[14] S. Khan et al. "Femtosecond Undulator Radiation from Sliced Electron Bunches," *Phys. Rev. Lett.* 97, 074801 (2006)

[15] K. Holldack et al. “Femtosecond Terahertz Radiation from Femtoslicing at BESSY” *Phys. Rev. Lett*. 96, 054801 (2006)

[16] J. Bahrdt et al., *Nucl. Instr. and Meth. in Phys. Res. A*, 516 (2004) pp 575-585.

[17] J. Bahrdt, Proc. 28th International FEL Conference, Berlin, Germany, 2006 (to be published)

[18] S. Reiche et al, p. 2396, “Optimization of the LCLS X-ray FEL performance in the presence of strong undulator wake-fields”, *Proc. 2005 Particle Accelerator Conference*, Knoxville, TN, 2396 (2005).

[19] Michael Scheer, BESSY, private communication.

[20] K. Holldack, S. Khan, R. Mitzner, T. Quast, *Phys. Rev. STAB* **8**, 040704 (2005)

[21] K. Holldack, D.Ponwitz, “A dedicated THz beamline at BESSY”, Proc. Int.Conf. on Synchr. Rad. Instrum., *Proc. SRI 2006, Daegu*, Korea, AIP proc., in press.

[22] M. AboBakr, J. Feikes, K.Holldack, H.-W. Hübers, G. Wüstefeld, *Phys. Rev. Lett.* **88**, 254801 (2002).

[23] Kung, H. C. Lihn, H. Wiedemann, D. Bocek, *Phys. Rev. Lett.* **73** (7), 967 (1994).

[24] K. Holldack, J. Feikes, W. B. Peatman, *Nucl. Instr. Meth* **A** 467 (2001).

[25] A.A. Zholents, K. Holldack, *Proc. Int. Conf. on Free electron Lasers, FEL 06*, Berlin, 2006, submitted.

[26] A. Winter et al., “High-Precision Laser Master Oscillators for Optical Timing Distribution Systems in Future Light Sources”, *Proc. EPAC 2006*.

[27] A. Winter et al., “High-Precision optical synchronization systems for X-Ray Free Electron Lasers”, *Proc. of the FEL 2005.*

[28] J. Kim et al. “An Integrated Femtosecond Timing Distribution System for XFELS” *Proc. EPAC 2005*

[29] T. Schibli et al. *Optics Letters* 28, 947 (2003)

[30] M. Richter, A. Gottwald, U. Kroth, A.A. Sorokin, S.V. Bobashev, A. Shmaenok, J. Feldhaus, Ch. Gerth, B. Steeg, K. Tiedtke, R. Treusch , “Measurement of gigawatt radiation pulses from a vacuum and extreme ultraviolet free-electron laser”, *Appl. Phys. Lett.*, **83**, 2970-2972, (2003).

[31] R. Mitzner, M. Neeb, T. Noll, N. Pontius and W. Eberhardt, “An X-ray autocorrelator and delay line for the VUV-FEL at TTF/DESY”, *Proc. SPIE 59200D* (2005).

[32] H. Chapman et al., "Femtosecond diffractive imaging with a soft-X-ray free-electron laser”, UCRL-JRNL-219848, http://arxiv.org/PS_cache/physics/pdf/0610/0610044.pdf